



# Bantam Lake

## 2020 Water Quality Monitoring

Prepared for the  
Bantam Lake Protective Association  
Morris, CT  
January 9, 2021

## EXECUTIVE SUMMARY

Aquatic Ecosystem Research (AER) was engaged by the Bantam Lake Protective Association to conduct monthly water quality monitoring and biweekly cyanobacteria monitoring from April through October of 2020 at two sites on Bantam Lake. Two additional sites were also visited during each sampling event where profile data (temperature, oxygen, etc.) and Secchi disk transparency data were collected. Supplemental data were also collected by James Fischer from the White Memorial Environmental Center; those data were also utilized in this analysis.

- Water column depth at the four sites was an important variable impacting stratification and other water quality variables.
  - The water column at the deepest site – the approximately 8m Center Lake site – was stratified from late May through early September.
    - Anoxic conditions were more prevalent at the CL site than at any other site.
    - Oxidation reduction potential (ORP) of <200mV and elevated specific conductances were observed in the CL hypolimnion often and were different compared to the other sites.
    - Hypolimnetic total phosphorus, TKN, ammonia, manganese, ferrous iron, and alkalinity were all higher at CL than other sites, particularly between July through September.
  - Two shallower sites of approximately 6m of depth – the North Bay and Folly Point sites – were found to be stratified from late May through late July/early August and then experienced intermittent stratification and mixing.
    - Oxygen concentrations of <1mg/L were observed at 6m of depth for much of the season and at 5m of depth from mid-June through to late August.
    - Hypolimnetic measurements of ORP >200mV – when ferric iron is used in cellular respiration and phosphorus becomes soluble – were observed but only intermittently.
    - Hypolimnetic total phosphorus, TKN, ammonia, manganese, ferrous iron, and alkalinity were intermittently high at the NB site but lower than those at the CL site; particularly, from July through August.
  - The only consecutive sampling events when the 4m water column of the South Bay site was stratified occurred in June; afterwards the water column was mostly mixed but was found to be stratified on one visit in July and one in August.
    - Anoxic conditions and ORP levels <200mV were observed occasionally at this site.
  - Stratification also appears to play a role in the distribution of Cyanobacteria in the water column.



- Algal productivity in the epilimnion was highest in early June and after mid-July.
  - A surface bloom of Cyanobacteria was observed on June 1<sup>st</sup>; it was principally comprised of *Aphanizomenon* spp.
  - High algal productivity and bloom conditions were observed frequently after mid-July; but those were principally comprised of *Dolichospermum* spp.
    - Low Secchi transparency measurements corresponded with high productivity and bloom conditions.
      - Forty-two of the 92 Secchi disk measurements were <2m, which were indicative of eutrophic status, and occurred in early June and after mid-July.
    - Chlorophyll-*a* concentrations and relative phycocyanin concentrations were not as predictive.
      - This may be due to sampling techniques. Samples for chlorophyll-*a* and relative phycocyanin concentrations were integrations of the top 3m of the water column, which may underestimate biomass if much of the Cyanobacteria is at the surface.
- Cyanobacteria cell concentrations throughout the season were largely characteristic of Visual Rank Category 2 (between 20,000 and 100,000 cells/mL).
  - The highest cell concentrations were from samples collected on June 1<sup>st</sup> and August 21<sup>st</sup> and 23<sup>rd</sup>.
    - Copper sulfate treatments occurred on August 6<sup>th</sup> and August 24<sup>th</sup> with the latter treatment effectively reducing cell concentrations, but only for a short period of time. By early September, cell concentrations returned to high levels.
  - Higher Cyanobacteria cell concentrations appeared to occur at or below the thermocline while the lake was stratified in July determined by relative phycocyanin concentrations.
  - An end of season sampling of the surface bloom resulted in cell concentrations of >400,000 cells/mL which was an order of magnitude higher than concentration estimated from the 3m-integrated samples.
  - Microcystin – the most common cyanotoxin – was measured by WCSU researchers in integrated samples collected biweekly at the NB and CL sites with all concentrations ≥1µg/L. The State recommends a threshold of 8µg/L.
- Nutrient concentrations in the epilimnion were generally characteristic of mesotrophic or late mesotrophic conditions.
  - The highest total phosphorus concentrations in the epilimnion were measured in samples collected in late April and mid-October.
    - The late April concentrations were assessed before stratification and internal loading of phosphorus from the bottom sediments.

- The mid-October concentrations followed loading from the sediments while the lake was stratified, anoxia present at the depths nearest the sediments, and mixing of the water column.
  - Nitrogen concentrations in the epilimnion were also mesotrophic in nature.
    - These concentrations trended up during the course of the season and reached maximum levels by mid-October following mixing.
- Nutrient concentrations in the hypolimnion became elevated once the lake stratified.
  - Total phosphorus levels were elevated in July and August at the NB site, in June through September at the CL site.
    - Those elevated levels could support algal productivity characteristic of highly eutrophic conditions.
    - Those elevated levels were concurrent with elevated ferrous iron, alkalinity and specific conductance, and low ORP in the hypolimnion linking phosphorus loading from the sediments.
  - Hypolimnetic total Kjeldahl nitrogen (TKN) also increased from late April through August 11<sup>th</sup> with much of that due to increasing ammonia.
    - Ammonia loading in the hypolimnion was a result of nitrate reduction in the anoxic sediments.
    - TKN was the equivalent of total nitrogen with one exception of September 9<sup>th</sup> in the hypolimnion of the CL site where nitrate was detected.
- Total nitrogen to total phosphorus ratios in the epilimnion were characteristic of phosphorus limitation.
  - In the hypolimnion, particularly at the CL site, the ratio after mid-July was characteristic of nitrogen limitation.
    - Formation of heterocysts, the specialized cells observed in *Dolichospermum spp.*, where nitrogen fixation occurs, increased after mid-July.
      - Coupled with our finding that highest concentrations of relative phycocyanin were at or below the thermocline where conditions are more nitrogen limited, we hypothesize that late season bloom conditions have their origins at lower depths in late-June and July.
- Other water quality characteristics and their implications on Cyanobacteria productivity are discussed as are recommendations for the 2021 season.



## TABLE OF CONTENTS

Executive Summary.....	2
Introduction .....	9
Historical Water Quality Studies.....	9
Current Water Quality Concerns .....	10
Methods.....	10
Monthly Water Quality Monitoring.....	10
Cyanobacteria Monitoring .....	11
Additional Data Collections.....	12
Mixing and Stratification .....	12
Database.....	12
Temperature and Oxygen Profiles .....	15
Oxidation-Reduction Potential .....	19
Biological and Nutrient Assessment .....	21
Secchi Disk Transparency.....	21
Chlorophyll-a Concentrations .....	22
Relative Phycocyanin Concentrations.....	23
Total Phosphorus Concentrations.....	24
Nitrogen Concentrations.....	25
Pelagic Algae Community, Cyanobacteria, and Cyanotoxins.....	27
Relative Phycocyanin Profiles .....	30
Microcystin Monitoring .....	31
Chemical Assessment.....	34
Specific Conductance.....	34
Iron and Manganese.....	37
Alkalinity and pH.....	38
Base Cations and Chloride .....	40
Major Findings.....	43
Trophic Status .....	43
Internal Loading and Cyanobacteria Dynamics.....	44
Allochthonous Phosphorus and Cyanobacteria Dynamics.....	47
Nitrogen, Limiting Nutrients, and Cyanobacteria.....	47



Other Environmental Factors and Cyanobacteria .....	48
Recommendations .....	51
References .....	53

## LIST OF FIGURES

Figure 1. Reconstruction of Bantam Lake trophic status between <i>ca</i> 1857 and <i>ca</i> 1991. .....	10
Figure 2. Locations of the sampling sites on Bantam Lake during the 2020 season... 13	
Figure 3. Temperature (top) and oxygen (bottom) isopleth diagrams for the North Bay (Site 1) and Center Lake (Site 2) sites in 2020 .....	16
Figure 4. Temperature (top) and oxygen (bottom) isopleth diagrams for the Folly Point (Site 3) and South Bay (Site 4) sites in 2020 .....	17
Figure 5. Oxidation-reduction potential (ORP) isopleth diagrams in millivolts (mV) the North Bay (Site 1), Center Lake (Site 2), Folly Point (Site 3) and South Bay (Site 4) in 2020.....	20
Figure 6. Secchi transparency measurements taken at the North Bay (NB), Center Lake (CL), Point Folly (PF), and South Bay (SB) sites during the 2020 season.. .....	22
Figure 7. Chlorophyll- <i>a</i> concentrations at the North Bay (NB) and Center Lake (CL) sites measured in 2020.....	22
Figure 8. Average relative phycocyanin concentrations from measurements taken in the top three meters of the water column at the North Bay (NB), Center Lake (CL), Point Folly (PF), and South Bay (SB) sites during the 2020 season.....	23
Figure 9. Total phosphorus (Phos.) concentrations in the epilimnion (Epi), metalimnion (Meta), and hypolimnion (Hypo) of the North Bay and Center Lake sites during the 2020 season.....	24
Figure 10. Top: Total Kjeldahl nitrogen (TKN) concentrations in the epilimnion (Epi), metalimnion (Meta), and hypolimnion (Hypo) at the North Bay (NB) and Center Lake (CL) sites in 2020. Bottom: TKN with the ammonia (NH <sub>4</sub> ) component displayed in the hypolimnion of the NB and CL sites in 2020.....	26
Figure 11. Cyanobacteria cell concentrations at the North Bay (NB) and Center Lake (CL) sites in 2020.....	28
Figure 12. Micrographs of specimens of algae genera collected from Bantam Lake in 2020.....	32
Figure 13. Isopleths of relative phycocyanin concentrations at the North Bay (Site 1), Center Lake (Site 2), Folly Point (Site 3), and South Bay sites in 2020 .....	33



Figure 14. Isopleths of specific conductance (SpC) at the North Bay (Site 1), Center Lake (Site 2), Folly Point (Site 3), and South Bay sites in 2020 .....	35
Figure 15. Results of ANOVA using specific conductance measurements at each depth during the 2020 season. Error bars represent on standard deviation.....	36
Figure 16. Concentrations of iron in the epilimnion (Epi) and hypolimnion (Hypo) of the North Bay (NB; top) and Center Lake (CL; bottom) sites in 2020.....	37
Figure 17. Concentrations of manganese in the epilimnion (Epi) and hypolimnion (Hypo) of the North Bay (NB) and Center Lake (CL) sites in 2020.....	38
Figure 18. Alkalinity in the epilimnion (Epi), metalimnion (Meta), and hypolimnion (Hypo) of the North Bay (NB) and Center Lake (CL) sites in 2020.....	39
Figure 19. pH levels in the epilimnion (Epi) and hypolimnion (Hypo) at the North Bay (NB), Center Lake (CL), Folly Point (FP), and South Bay (SB) sites in 2020. ....	40
Figure 20. Average base cation, chloride and alkalinity ion concentrations at the North Bay (left) and Center Lake (right) sites in meq/L during the 2020 season.....	41
Figure 21. Photographs of the Cyanobacteria surface scum at Bantam Lake taken on September 21, 2020.....	44
Figure 22. Results of analyses of the mass of phosphorus at each stratum of the water column (left) or for the entire water column (right) during the 2018, 2019, and 2020 sampling seasons.....	46
Figure 23. Epilimnetic and hypolimnetic pH averages for the 2020 season in the epilimnion (Epi) and hypolimnion (Hypo) of the North Bay (NB), Center Lake (CL), Folly Point (FP), and South Bay (SB) sites. Error bars represent one standard deviation.....	49
Figure 24. Maximum RTRM scores plotted over time in the water column of the North Bay (NB), Center Lake (CL), Folly Point (FP), and South Bay (SB) sites during the 2020 season.....	50
Figure 25. Ferrous iron concentrations in the hypolimnion of the North Bay and Center Lake sites in the 2018, 2019, and 2020 seasons. Data not available for August 26 – October 7, 2019. ....	51

## LIST OF TABLES

Table 1. Summary of data collections for Bantam Lake in 2020 used in this report .....	14
Table 2. List of genera by taxonomic group identified in samples collected at Bantam Lake in 2020. ....	30
Table 3. Microcystin concentrations in µg/L in samples collected at Bantam Lake in 2020.....	31

Table 4. Base cations potassium (K <sup>+</sup> ), sodium (Na <sup>+</sup> ), calcium (Ca <sup>2+</sup> ), magnesium (Mg <sup>2+</sup> ), chloride (Cl <sup>-</sup> ), and alkalinity ions (Alk) at the North Bay (NB) and Center Lake (CL) sites in 2020 in both mg/L and meq/L.....	42
Table 5 . Trophic classification criteria used by the Connecticut Experimental Agricultural Station (Frink and Norvell 1984) and the CT DEP (1991) to assess the trophic status of Connecticut lakes .....	43
Table 6. Redfield ratios in µg/L at the North Bay (NB) and Center Lake (CL) sites in the epilimnion (Epi), metalimnion (Meta), and hypolimnion in 2020.....	48



## INTRODUCTION

Bantam Lake is a 966-acre waterbody located in the Towns of Litchfield and Morris, CT and is the largest natural lake in Connecticut. Geologically, it is situated in the Western Uplands of Connecticut (Bell 1985, Canavan & Siver 1995) that has an erosion resistant, crystalline bedrock geology that is comprised of schists, gneiss, granite gneiss, and granofels (Healy & Kulp 1995).

The watershed of Bantam Lake is 20,218 acres resulting in a watershed to lake ratio of approximately 21. In a 1995 survey, land use was characterized as mainly deciduous forest and agriculture lands with smaller areas of medium-density residential land use, wetlands, and coniferous forests (Healy & Kulp 1995). Much of the shoreline is lined with homes, beaches, and several camps. There is also open space along the northern shoreline, which is owned by the White Memorial Foundation.

### *Historical Water Quality Studies*

In situ studies of water quality for Bantam Lake date back as far as the 1930s and occurred several times over the next 70 years as part of statewide surveys of Connecticut Lakes (e.g., Deevey 1940, Frink & Norvell 1984, Canavan & Siver 1994, 1995). In the early 1990s, a paleolimnological study on Bantam Lake's historical water quality was conducted (Siver 1992). This study applied statistical inference models developed from the remains of fossil bearing algal layered chronologically in sediment cores to estimate changes in water quality over time (e.g., trophic level, conductivity levels, and pH, over time; Siver 1993, Siver and Marsicano 1996). The sediment core strata were dated with isotope dating methods to provide a temporal context to reconstructed water quality conditions (Fig. 1).

The historical trophic condition of Bantam Lake was expressed as a trophic score developed by the integration of total phosphorus, total nitrogen, chlorophyll-*a*, and Secchi disk into one "trophic score" using principal component analysis (Siver and Marsicano 1996). The oldest sediments at the bottom of the 42cm-long core dated back to *ca* 1857. The fossil assemblages there, and up to the assemblages in sediments that dated to *ca* 1898, reflected oligotrophic / early mesotrophic condition (Fig. 1).

The trophic status began to shift after *ca* 1900 and by *ca* 1926, Bantam Lake was mesotrophic. Trophic state continued to steadily increase but was still within the mesotrophic range through *ca* 1946. Between *ca* 1946 and *ca* 1964, the rate of eutrophication increased resulting in eutrophic conditions where it remained to *ca* 1991, i.e., the top layer of the sediment core.

Bantam Lake has continued to exhibit eutrophic characteristics with high levels of algal productivity one of the primary management concerns. High concentrations of cyanobacteria and bloom-like conditions are common between the midsummer and fall portions of the recreational season.

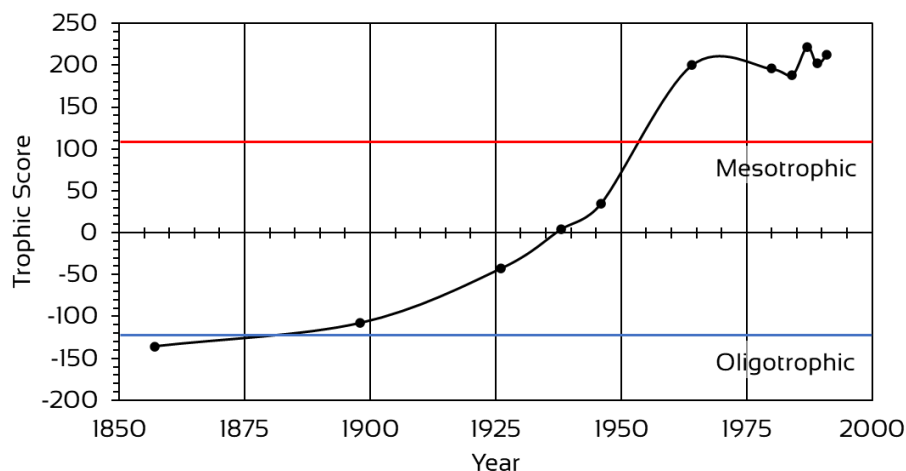


Figure 1. Reconstruction of Bantam Lake trophic status between *ca* 1857 and *ca* 1991. The blue horizontal line represents the division between oligotrophic and mesotrophic lakes; and the red horizontal line represents the division between mesotrophic and eutrophic lakes based on a trophic score (Siver and Marsicano 1996).

### Current Water Quality Concerns

Harmful algal blooms or HABs, have become a key issue in lake management over the last 20 year because of the risk they present to ecosystem and public health. In addition to depletion of oxygen from the water column following a bloom, many genera of cyanobacteria are toxigenic. The cyanotoxins are generally grouped into one of several categories: hepatotoxin that cause liver damage, neurotoxins that have been associated with neurological disorders like amyotrophic lateral sclerosis (ALS), and others in groups classified as dermatoxins, cytotoxins, and endotoxins. The State of Connecticut provides a useful summary on cyanobacteria, the toxins they produce, and standards by which municipal health department can assess conditions at public beaches (CT DPH & CT DEEP 2019).

## METHODS

### Monthly Water Quality Monitoring

Four sampling sites (Fig. 2) were visited six times each between April and October of 2020. Inclement weather on the April 23<sup>rd</sup> sampling date precluded completing data collection. That data collection was completed on May 5<sup>th</sup> but will be discussed as if was collected on April 23<sup>rd</sup> for the purposes of this report. Other dates of data and water sample collections were: May 21<sup>st</sup>, June 17<sup>th</sup>, July 13<sup>th</sup>, August 11<sup>th</sup>, September 9<sup>th</sup> and October 19<sup>th</sup>. Sites were identified as North Bay (NB), Center Lake (CL), Folly Point (FP), and South Bay (SB). Maximum depths were approximately 6 meters (m), 8m, 6.5m, and 4.5m at the NB, CL, FP, and SB sites, respectively.

During each site visit, Secchi transparency was measured with a 26cm diameter Secchi disk. Additionally, vertical profile data for six parameters were collected using a Eureka Manta II multiprobe sensor. Profiled data were measured at 0.5m from the surface and at one-meter intervals to 0.5m above the bottom, and included the following variables: temperature (°C), dissolved oxygen (mg/L), percent oxygen saturation (% O<sub>2</sub>), specific conductance (µS/cm), pH, oxidation-reduction potential, and relative cyanobacteria concentration.

Water samples were collected at NB and CL during site visits and analyzed for the variables listed in Table 1 by a State-certified laboratory with the exception of algae samples, which were analyzed by AER. Water samples were collected using two different methods and at several depths in the water column. For nutrient and alkalinity analyses, samples were collected with a horizontal Van Dorn water sampler at 1m below the surface (epilimnion), at approximately 0.5m above the sediment water interface (hypolimnion), and at the thermocline, which was determined using the vertical temperature profiles collected at each site on each sample date. For iron (Fe) and manganese (Mn), samples were collected with the Van Dorn sampler at 1m below the surface and 0.5m above the sediment water interface. For base cations of sodium (Na<sup>+</sup>), potassium (K<sup>+</sup>), calcium (Ca<sup>2+</sup>), magnesium (Mg<sup>2+</sup>), and the anion chloride (Cl<sup>-</sup>), samples were collected from 1m below the surface. All samples were kept on ice in a cooler until delivered to a State-certified lab for analyses.

For chlorophyll-*a*, a weighted tube sampler was used to collect and integrate water from the top three meters of the water column at the NB and CL sites. All samples were kept on ice in a cooler until delivered to a State-certified lab for analyses.

### *Cyanobacteria Monitoring*

Pelagic algae samples were collected on 19 different dates in 2020 (Table 1), including the dates water quality data and samples were collected. Although the sampling regime was originally designed as biweekly, weekly sampling occurred from June 1<sup>st</sup> through July 27<sup>th</sup> due to observed bloom conditions. Sampling events also occurred within days each other on August 23<sup>rd</sup> and August 26<sup>th</sup>, and on September 9<sup>th</sup> and September 11<sup>th</sup>. The reasoning for these frequent sampling events was also due to observable high concentrations of algae.

Samples for algal analyses were collected at the NB and CL sites by integrating the top three meters of the water column with a 3-meter-long sampling tube. Samples were treated with Lugols and kept on ice. Samples were treated with hydrostatic pressure back in the AER laboratory to collapse gas vesicles that might be making cells positively buoyant (Lawton et al. 1999).

If necessary, measured volumes of the preserved whole water samples were concentrated into smaller measured volumes with centrifugation and a vacuum pump / filtra-

tion flask system. This step was omitted when Cyanobacteria concentrations appeared high based on a visual assessment at the lake. A known portion of those concentrates or whole water samples were pipetted into a counting chamber and genus-level algal cell enumerations were performed by counting algae cells in a subset of fields within the counting chamber slide using an inverted Nikon Diaphot research microscope. Those counts were then corrected to be reflective of the whole sample.

Additionally, a 10µm mesh plankton net was used to collect a concentrated algal sample from within the top 3m of the CL water column. Those samples were examined and dominant genus photographed in the laboratory using a Wolfe Digivi™ CVM Microscope with Motic Images Plus 3.0 software.

During each algae sample collection visit, Secchi transparency and vertical profile data were collected at NB, CL, FP, and SB sites. A total of 19 samples for algal analyses were collected at the NB and CL sites in 2020.

### *Additional Data Collections*

In addition, Secchi transparency and profile data were collected by James Fischer, Director of Research for the White Memorial Conservation Center. The White Memorial Conservation Center is a partner and advisor to the Bantam Lake Protective Association. The data collected by Mr. Fischer facilitated greater temporal resolution in assessments of seasonal Secchi transparencies, and temperature/oxygen dynamics in the water column. Those data have been incorporated into the results and discussions below. Specific dates of AER's and Mr. Fischer's site visits and data collections are outlined in Table 1.

### *Mixing and Stratification*

Patterns of water column mixing and resistance to mixing (or stratification) were assessed using temperature profile data. Where temperature profile data was collected by both AER and Mr. Fischer on the same date, AER data was used. Resistance to mixing, which is an assessment of the ability of two different water volumes – that differ in temperature and density – to mix, was calculated using the Relative Thermal Resistance to Mixing (RTRM) formula:  $(D_1 - D_2)/(D' - D^0)$ , where  $D_1$  is the density of upper water volume,  $D_2$  is the density of the lower water volume,  $D'$  is the density of water at 5°C, and  $D^0$  is the density of water at 4°C.

### *Database*

All water quality data was provided to the BLPA in a supplemental Excel database.

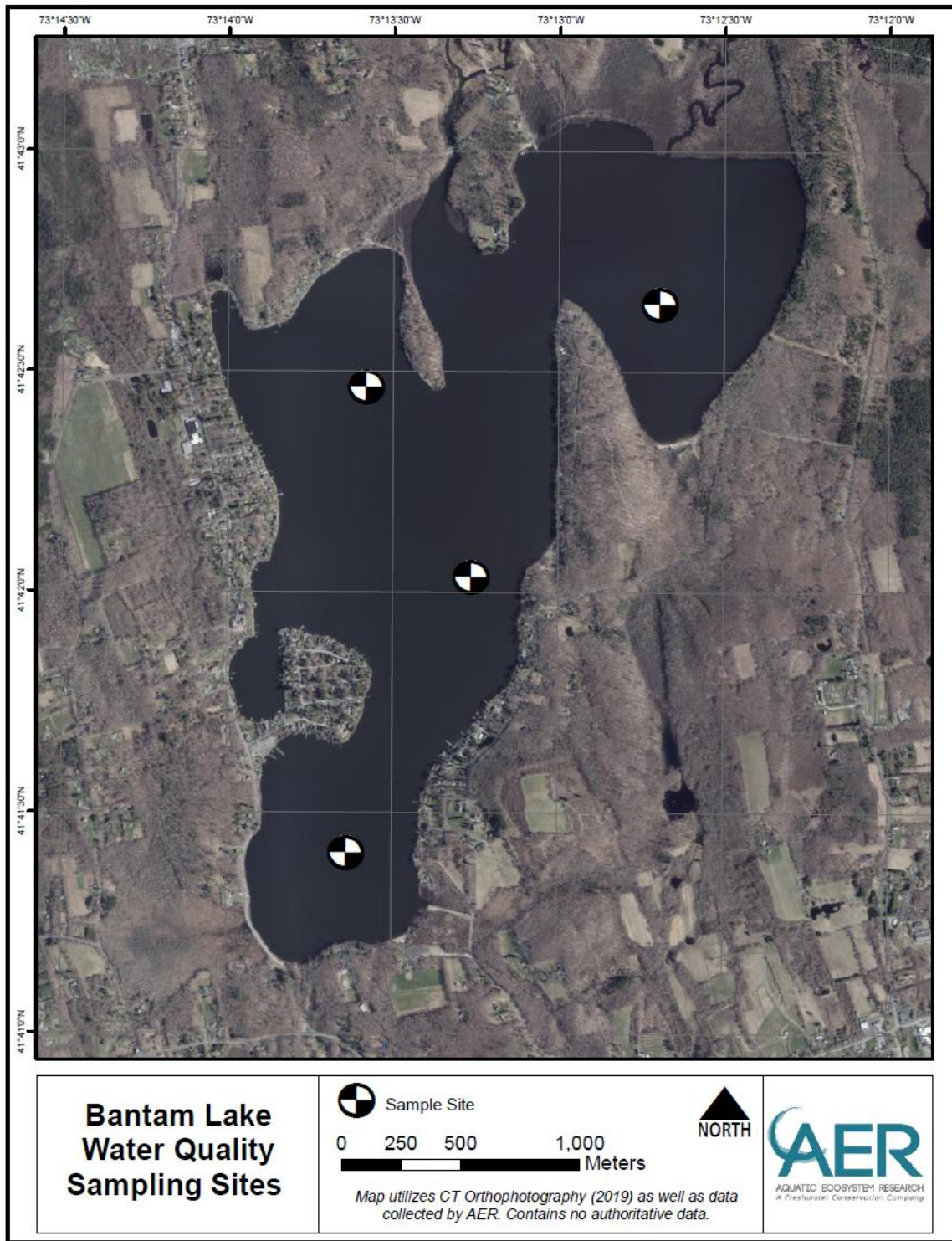


Figure 2. Locations of the sampling sites on Bantam Lake during the 2020 season. NB = North Bay Site, FP = Folly Point Site, CL = Center Lake Site, and SB = South Bay Site.

Table 1. Summary of data collections for Bantam Lake in 2020 used in this report. NB = North Bay Site, CL = Center Lake Site, FP = Folly Point Site, and SB = South Bay Site. Chl-*a* = chlorophyll-*a*.

2020 Dates	Profiles and Secchi	Algae	Nutrients & Alkalinity	Iron & Manganese	Chl- <i>a</i> , Cations, Chloride
23-Apr-20	NB	NB, CL	NB, CL	NB, CL	NB, CL
29-Apr-20*	NB, CL				
5-May-20	NB, CL	NB, CL			
14-May-20*	NB, CL, FP, SB				
21-May-20	NB, CL, FP, SB	NB, CL	NB, CL	NB, CL	NB, CL
28-May-20*	NB, CL, FP, SB				
1-Jun-20	NB, CL, FP, SB	NB, CL			
9-Jun-20	NB, CL, FP, SB	NB, CL			
17-Jun-20	NB, CL, FP, SB	NB, CL	NB, CL	NB, CL	NB, CL
24-Jun-20	NB, CL, FP, SB	NB, CL			
1-Jul-20	NB, CL, FP, SB	NB, CL			
6-Jul-20	NB, CL, FP, SB	NB, CL			
13-Jul-20	NB, CL, FP, SB	NB, CL	NB, CL	NB, CL	NB, CL
20-Jul-20*	NB, CL, FP, SB				
27-Jul-20	NB, CL, FP, SB	NB, CL			
5-Aug-20*	NB, CL, FP, SB				
11-Aug-20	NB, CL, FP, SB	NB, CL	NB, CL	NB, CL	NB, CL
19-Aug-20*	NB, CL, FP, SB				
21-Aug-20*	NB, CL				
23-Aug-20	NB, CL	NB, CL			
26-Aug-20	NB, CL, FP, SB	NB, CL			
31-Aug-20*	NB, CL, FP, SB				
7-Sep-20*	NB, CL				
9-Sep-20	NB, CL, FP, SB	NB, CL			
11-Sep-20	NB, CL, FP, SB	NB, CL	NB, CL	NB, CL	NB, CL
21-Sep-20	NB, CL, FP, SB	NB, CL			
5-Oct-20	NB, CL, FP, SB	NB, CL			
19-Oct-20	NB, CL, FP, SB	NB, CL	NB, CL	NB, CL	NB, CL

\* Data collections by James Fischer of the White Memorial Conservation Center. All others by AER.



## TEMPERATURE AND OXYGEN PROFILES

Water quality variables measured throughout the water column are provided in the supplement to this report. We have displayed many of those data below as isopleths where a variable (e.g., temperature) is displayed as shades of colors throughout the water column at each depth and for all dates data were collected. Values are then interpolated between depth and dates. Variables of same value (and color) are connected between dates regardless of depth to create a theoretical representation of changes throughout the water column over time. Temperature profile data provides a means for assessing thermal differences and to determine where the water column is or is not vertically mixing due to temperature/density gradients. In shallow lakes, stratification can occur; but it may be short in duration as energy from wind can mix the water column. In deeper lakes, a middle transitional layer (aka metalimnion) separates the upper warmer layer (aka epilimnion) from lower, colder waters below (aka hypolimnion). Within the metalimnion resides the thermocline, which is the layer between two strata where temperature/density differences are greatest resulting in the greatest Relative Thermal Resistance to Mixing (RTRM). Those conditions will normally persist in deep lakes for the entire summer and early fall until thermal differences degrade and the lake mixes.

Coollest temperatures of the sampling season occurred between late April and mid-May while the water column was completely mixed (Figs. 3 & 4). By May 21<sup>st</sup>, as temperatures in the upper strata of the water column warmed to 15°C, stratification was first observed at the deeper NB, CL, and FP sites. Water temperatures within the shallower water column of the SB site likewise warmed to approximately 15°C; stratification was not observed at the SB site until June 9<sup>th</sup> when temperatures in the upper strata were between 21 and 22°C.

Depth of the water column and site location relative to wind fetch continued to influence the pattern of stratification at the four sites. At the deepest CL site, a thermocline was detected on consecutive visits until September 7<sup>th</sup>; the upper and lower boundaries of the metalimnion were not as consistently detected but were observed more consistently than observed at the other sites.

Patterns of stratification at the NB and FP sites were similar to each other, likely due to the sites being similar in depth. A thermocline was detected each visit at the NB site through July 27<sup>th</sup> and through August 11<sup>th</sup> at the FP site. The water column was mostly mixed afterwards with intermittent stratification (Figs. 3 & 4).

At the SB site, the only consecutive observations of a thermocline were between June 9<sup>th</sup> and June 27<sup>th</sup>. Additionally, a thermocline was detected on July 6<sup>th</sup> and August 11<sup>th</sup>. The SB site water column was mixed on all other sampling dates (Fig. 4).

By mid to late August, water temperatures began to cool and differences in temperature *within* the water column became smaller. By late September and for the remainder of the season, the water columns at all sites were nearly isothermal.



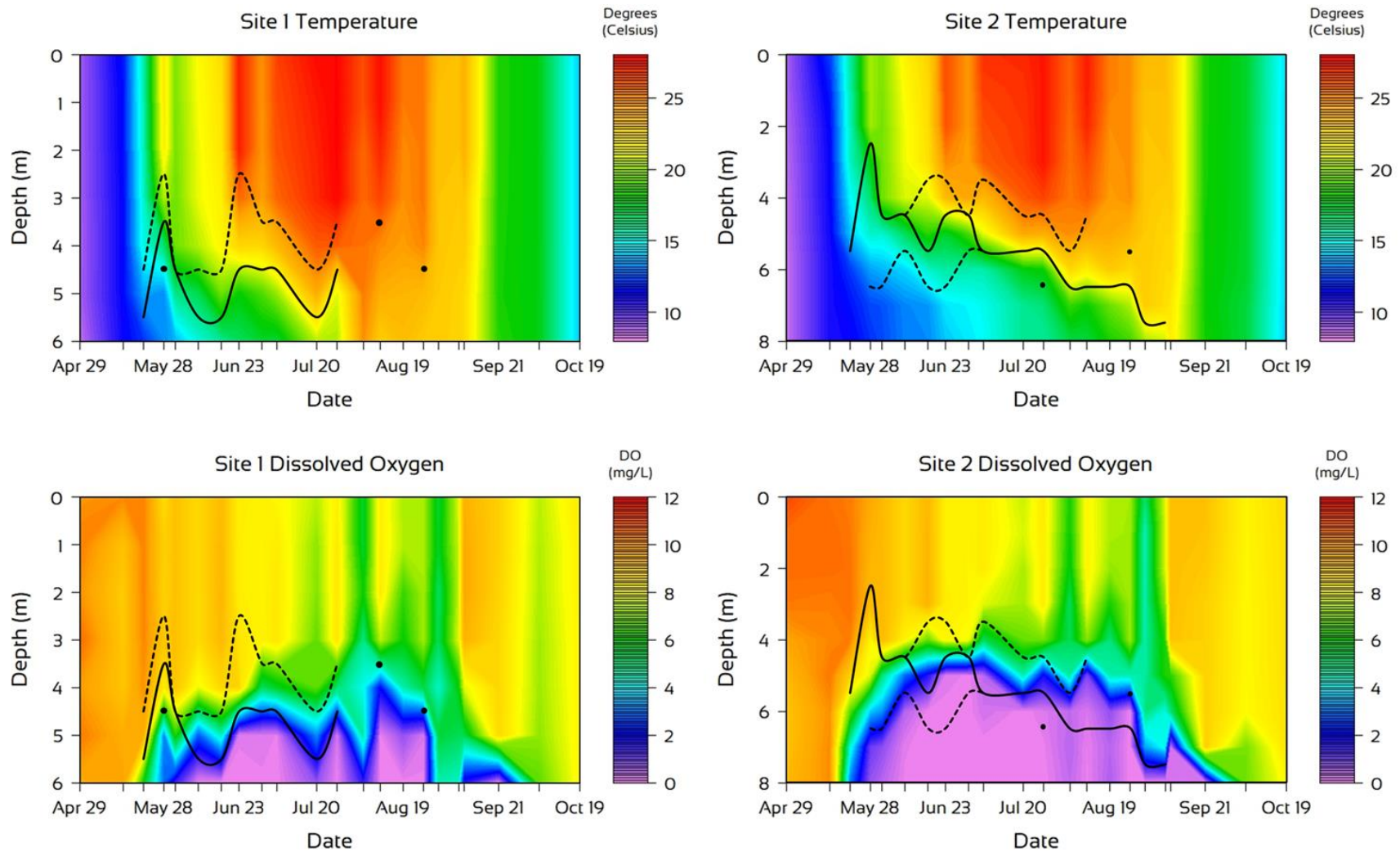


Figure 3. Temperature (top) and oxygen (bottom) isopleth diagrams for the North Bay (Site 1) and Center Lake (Site 2) sites in 2020. The dashed black line represents the upper or lower boundary of the metalimnion; the solid black line represents the thermocline.

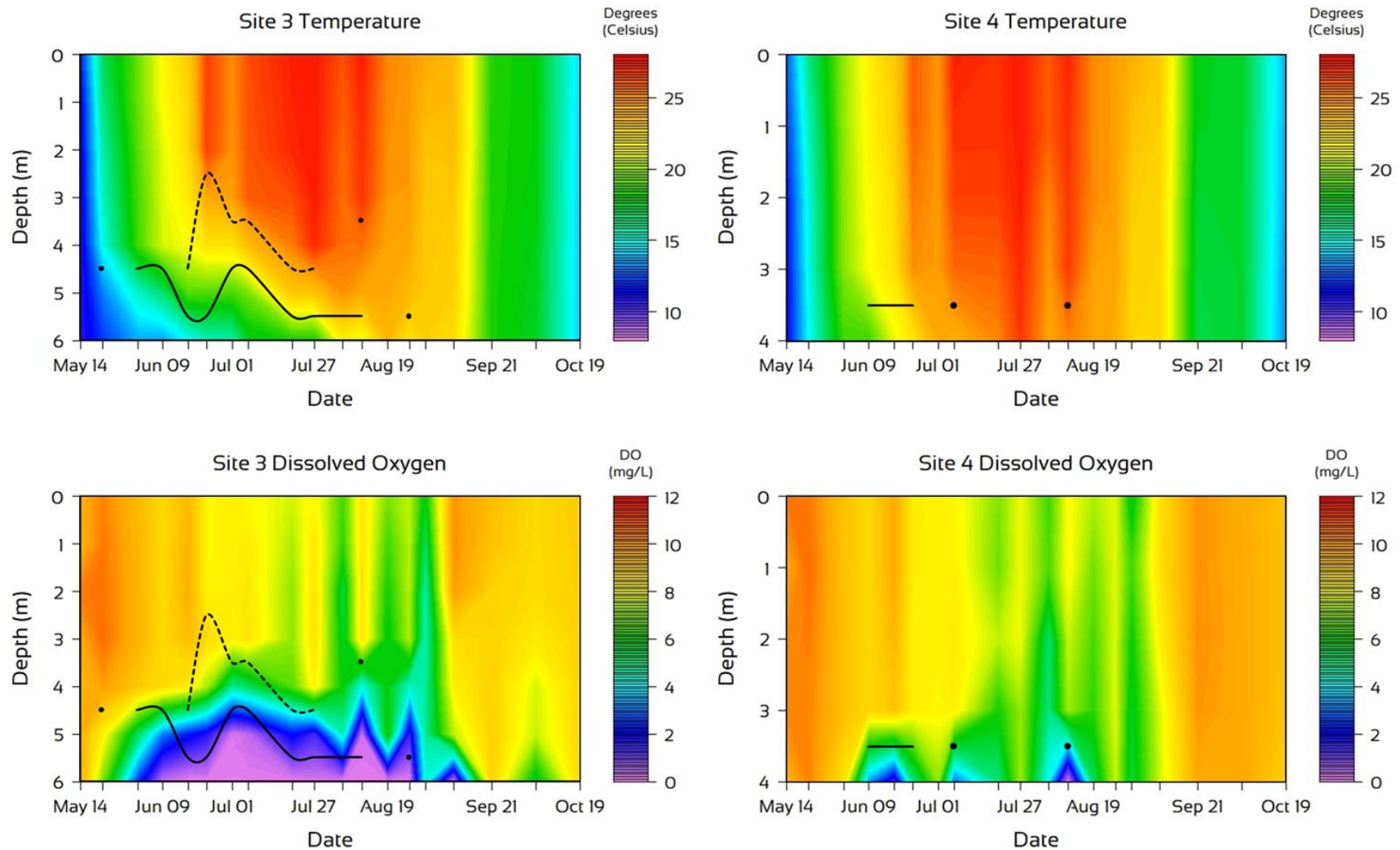


Figure 4. Temperature (top) and oxygen (bottom) isopleth diagrams for the Folly Point (Site 3) and South Bay (Site 4) sites in 2020. The dashed black line represents the upper or lower boundary of the metalimnion; the solid black line represents the thermocline.

An oxygen concentration of 5mg/L is generally considered the threshold for sustainable conditions for most aerobic organisms in freshwater systems. As concentrations drop below the threshold, conditions become stressful. Minimum oxygen requirements for fisheries in Connecticut's lakes and ponds range from 4 to 5mg/L for cold-water fish (e.g., trout), 2mg/L for cool-water fish (e.g., walleye), and 1 to 2mg/L for warm-water fish (e.g., bass and panfish; Jacobs and O'Donnell 2002).

Anoxic conditions at the bottom of the lake develop as oxygen is consumed in cellular respiration but not replenished because it cannot diffuse below the thermocline or diffuse to lowest depths at a rate that is greater than its consumption. Then metabolic pathways and the organisms change at those lower depths as elements other than oxygen are used for cellular respiration. Under those conditions, loading of phosphorus from the sediments to overlying waters can occur (see *Iron and Manganese* below).

Oxygen concentrations at all depths of all sites were >9mg/L through May 14<sup>th</sup>. By May 21<sup>st</sup>, at the NB, CL, and FP sites – when those water columns were first observed stratified – oxygen levels below the thermocline were reduced compared to those above (Figs. 3 & 4); the lowest concentration of 2.9mg/L was observed at the sediment/water interface of the CL site. A concentration of <1mg/L was measured for the first time on May 28<sup>th</sup> at the bottom (8m of depth) of the CL site.

The first observations of oxygen concentrations of <1mg/L at the NB and FP sites occurred on June 9<sup>th</sup>, at the sediment/water interface or at approximately 6m of depth. On that date, anoxic conditions (hereafter used interchangeably with <1mg/L, based on oxygen sensor margin of error) at the CL site were observed from 6 to 8m of depth; and, from 5 to 8m of depth on June 23<sup>rd</sup>. Anoxic conditions were also encountered at 5 and 6m of depth at the NB site; and, at 6m of depth at the FP site.

From July 1 through August 26<sup>th</sup>, an anoxic environment was observed from either 5 or 6m of depth to the bottom at the NB, CL, and FP sites. On August 31<sup>st</sup> and September 7<sup>th</sup>, only the very bottom (8m of depth) of the CL site was anoxic. Several days later, on September 9<sup>th</sup>, all strata had concentrations of >1mg/L. Anoxic conditions were again observed at the bottoms of the NB (6m of depth) and CL sites (8m of depth) on September 21<sup>st</sup>. This would mark the final time of the season that anoxic conditions were encountered; and by October 19<sup>th</sup>, all depths of all sites had concentrations of >8mg/L.

The SB site differed markedly from the other sites in that anoxic conditions were observed only on August 11<sup>th</sup> and only at the sediment/water interface (4m of depth). Oxygen at the bottom of the SB site was observed to have oxygen concentration <3mg/L on June 17<sup>th</sup> and July 6<sup>th</sup>. Those low oxygen events corresponded with sampling dates when a thermocline was detected at the SB site.

## OXIDATION-REDUCTION POTENTIAL

The oxidation-reduction potential (aka redox potential or ORP) in lakes refers to the oxidative or reductive state in a particular stratum of the water column; it can provide some insight as to whether phosphorus is changing from an insoluble particulate state in the sediments to a soluble state that readily diffuses to overlying waters and available to lentic algae if mixed into the photic zone (i.e., where algae can harvest it for growth). When ORP is  $\geq 200$  millivolts (mV) phosphate remains bound to iron; at ORP values of  $< 200$  mV, iron is reduced and the phosphate that is chemically bound to the iron becomes soluble (Søndergaard 2009). In some cases, a sudden mixing of phosphate-laden bottom waters to the upper reaches of the water column during a storm or wind event can trigger an algae bloom.

All sites exhibited some periods of time when ORP levels were  $< 200$  mV near the sediment-water interface. At the NB, FP, and SB sites, those conditions were generally limited to the stratum in the water column where data was collected above the sediments (Fig. 5). Those strata of the NB, FP, and SB sites exhibited the reduced conditions, but those conditions were intermittent and/or interrupted by periods where ORP at the bottom was  $> 200$  mV (e.g., August 11<sup>th</sup> at the NB and FP sites, or from June 23<sup>rd</sup> to July 27<sup>th</sup> at the SB site; Fig. 5). At the CL site, however, ORP measures of  $< 200$  mV near the bottom were observed consistently from June 9<sup>th</sup> through September 21<sup>st</sup>. Additionally, those conditions regularly occupied from 6m of depth to the bottom (or approximately 8m).

The ORP levels at all depths of all sites were  $> 200$  mV through Jun 1<sup>st</sup>. On June 9<sup>th</sup>, the top several meters of the CL, FP, and SB water columns had ORP measures between 170 and 200 mV; and, the 7 and 8m strata at the CL sites also had ORP levels of  $< 200$  mV. On June 17<sup>th</sup>, the ORP of the stratum nearest the bottom was highest at the FP site (56 mV) and lowest at the CL and SB sites with values of -128 and -157 mV, respectively. ORP levels of  $< 200$  mV were also recorded at the 6 and 7m strata at the CL site on that date.

On June 23<sup>rd</sup>, the bottom of the water column (6m) at the FP site, and from 5 to 8m of depth at the CL site exhibited ORP of  $< 200$  mV. On July 1<sup>st</sup> and 6<sup>th</sup>, the low ORP conditions ( $< 200$  mV) were observed at the bottom of the NB site and at the 7 to 8m strata of the CL site. On July 27<sup>th</sup>, low ORP was measured at the 5 to 6m strata of the NB site, the 6 to 8m strata of the CL site, at the 6m strata or bottom of the FP site, but not at the bottom of the SB site. Similar conditions were observed on August 26<sup>th</sup>. Between the July 27<sup>th</sup> and August 26<sup>th</sup>, the bottom of the SB site was highly reduced (-119 mV on August 11<sup>th</sup>).

Only the 7 and 8m strata of the CL site exhibited low ORP on September 9<sup>th</sup>. Highly reduced conditions were again encountered (-54 mV and -148 mV) at the NB and CL sites respectively, on September 21<sup>st</sup>. These would be the last observations of low ORP at any site for the remainder of the season.





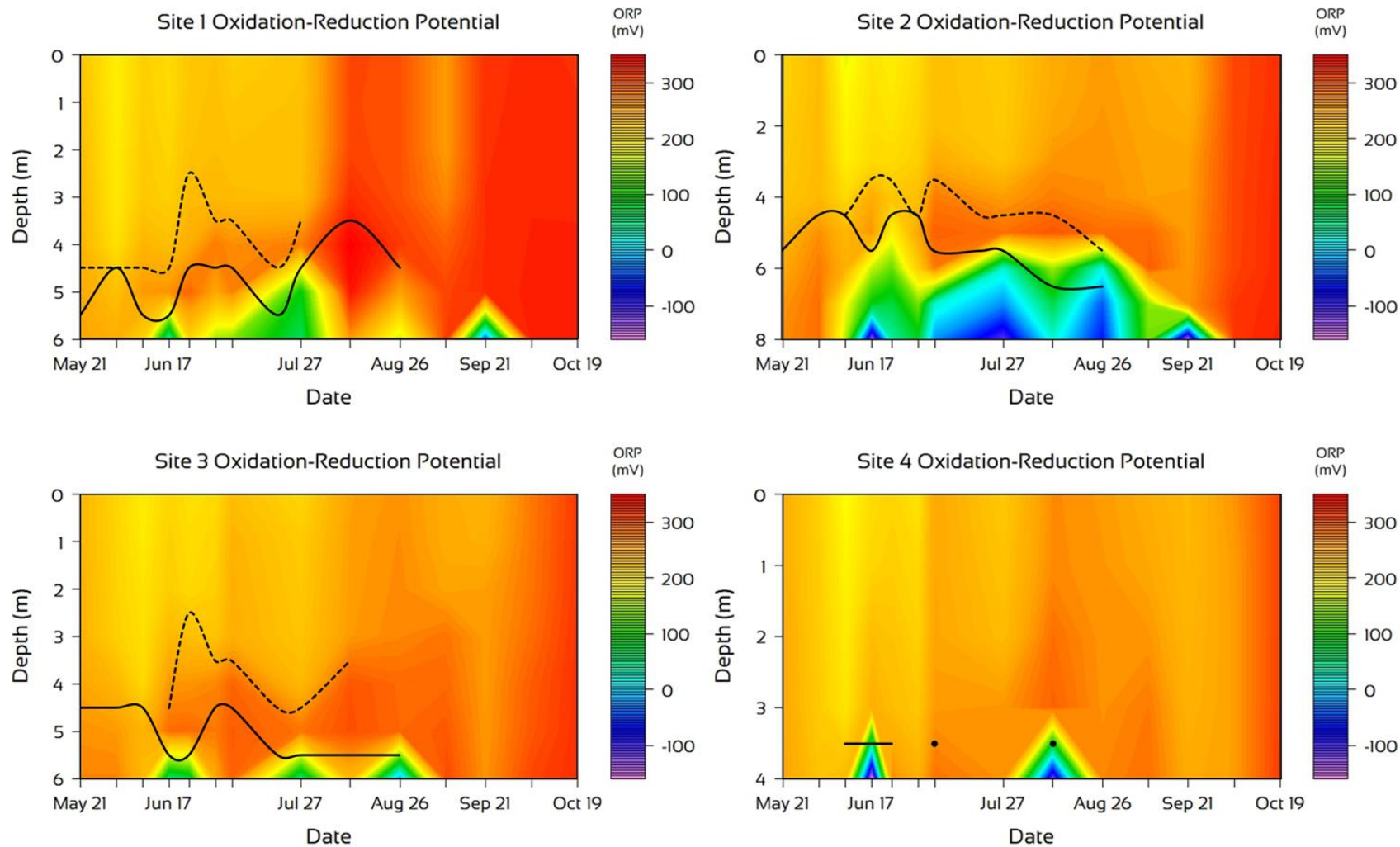


Figure 5. Oxidation-reduction potential (ORP) isopleth diagrams in millivolts (mV) the North Bay (Site 1), Center Lake (Site 2), Folly Point (Site 3) and South Bay (Site 4) in 2020. The dashed black line represents the upper or lower boundary of the metalimnion; the solid black line represents the thermocline.

## BIOLOGICAL AND NUTRIENT ASSESSMENT

### *Secchi Disk Transparency*

Secchi disk transparency is a measure of how much light is transmitted through the water column. That transmission is influenced by a number of variables including the amounts of inorganic and organic particulate material in the water column that absorbs or reflects light. In the open water environment, Secchi disk transparency is inversely related to algal productivity (i.e., the more algae in the water, the less Secchi transparency).

Light in lakes is important for several reasons including its impact on pelagic photosynthesis and algal productivity. As light diminishes with depth, so too does maximum photosynthetic activity. As photosynthesis decreases with depth, the observer encounters a stratum where oxygen production from photosynthesis equals oxygen consumed via respiration. That is referred to as the compensation depth; it is estimated by multiplying the Secchi disk transparency by 2.

Data collected by both AER and by WMCC were pooled in this assessment. Data was collected at the NB and CL sites on 26 different days; at the FP and SB sites, clarity was measured on 20 different days. A total of 92 measurements were made lake wide between April 23<sup>rd</sup> and October 19<sup>th</sup>.

The averages at the NB, CL, and FP sites were 2.18, 2.16, and 2.14 meters (m), respectively. The season average at the SB site was 1.91m. Differences among the season averages at the four sites were not significant ( $p > 0.05$ ). The season average for the lake was 2.11m.

The lake averages from April 23<sup>rd</sup> through July 20<sup>th</sup> were between 2 and 3m with three exceptions. First, the average on May 3<sup>rd</sup> was 3.05m but was based on one measurement (CL). Secondly, the lake average on June 1<sup>st</sup> was 1.53m when a cyanobacteria bloom comprised mostly of *Aphanizomenon spp.* was encountered. The third exception was on June 9<sup>th</sup>, when average Secchi disk transparency recovered after the bloom to 3.15m. By July 20<sup>th</sup>, the lake average decreased to 2.37m.

Between July 27<sup>th</sup> and October 19<sup>th</sup>, the lake averages were all between 1 and 2m with the exception of the August 11<sup>th</sup> average of 2.02m. Secchi transparency gradually decreased after July 27<sup>th</sup> with two exceptions. The first occurred between August 5<sup>th</sup> and August 11<sup>th</sup> when the lake average increased from a season low of 1.32m to 2.02m. The second occurred between August 23<sup>rd</sup> and August 26<sup>th</sup> when the lake average increased from 1.54m to 1.92m. In both instances, the increases followed an algae management initiative with copper sulfate. The first application was on August 6<sup>th</sup>; the second occurred on August 24<sup>th</sup> (Fig. 6).

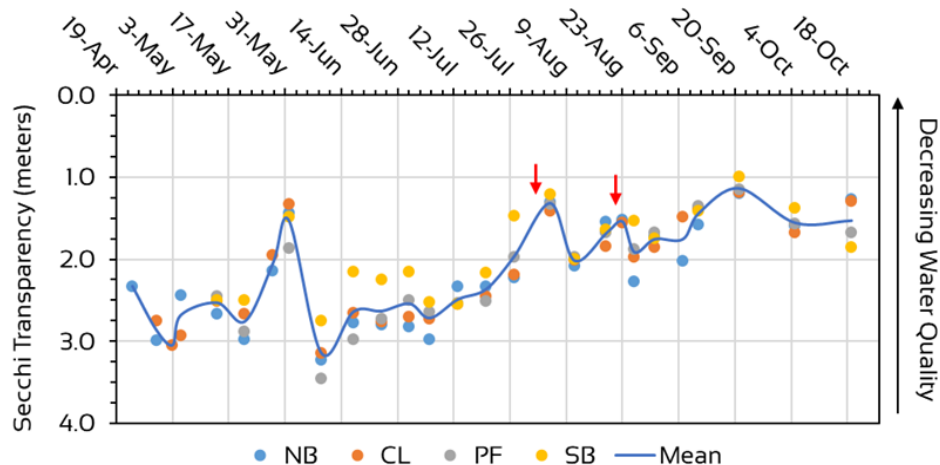


Figure 6. Secchi transparency measurements taken at the North Bay (NB), Center Lake (CL), Point Folly (PF), and South Bay (SB) sites during the 2020 season. The red arrows indicate the timing of the copper sulfate treatments that occurred on August 6<sup>th</sup> and August 24<sup>th</sup>.

### Chlorophyll-a Concentrations

Chlorophyll-a is a photosynthetic pigment common to all freshwater algae, including Cyanobacteria and is used as a surrogate measurement for algal biovolume in the water. Samples collected monthly from the NB and CL sites were an integration of the top three meters of the epilimnion where productivity in the water column is greatest.

The season averages at the NB and CL sites were 8.9 and 8.1 µg/L, respectively, and were not significantly different ( $p > 0.05$ ). In general, lowest concentrations were measured early in the season and gradually increased over time to highest levels measured on September 9<sup>th</sup> and October 19<sup>th</sup> (Fig. 7). It is worth noting that the October 19<sup>th</sup> concentration at the NB site is nearly double that of the CL site.

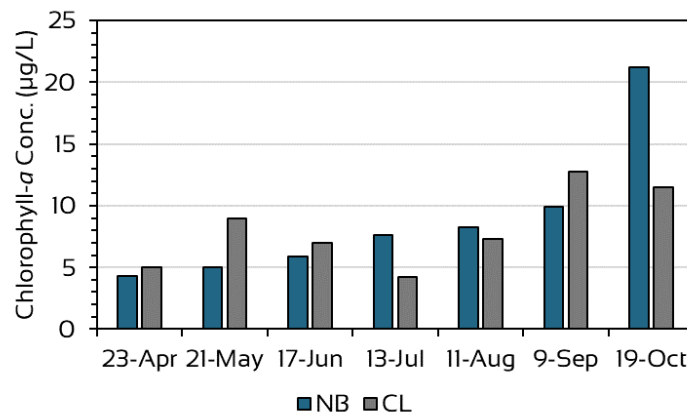


Figure 7. Chlorophyll-a concentrations at the North Bay (NB) and Center Lake (CL) sites measured in 2020.



### Relative Phycocyanin Concentrations

In addition to assessing the relative concentrations of phycocyanin throughout the water column (see *Relative Phycocyanin Profiles* below), readings from the top three meters of the water column were averaged for each date at each of site (Fig. 8). Those averages were used as another variable in the characterization of Cyanobacteria productivity in the upper strata of the lake.

Relative phycocyanin concentrations were low ( $<5\mu\text{g/L}$ ) from mid-April to mid-July. Exceptions included readings on June 1<sup>st</sup> when the first Cyanobacteria bloom was detected; and, to a lesser degree, on July 1<sup>st</sup> when average relative concentrations at several sites were just above  $5\mu\text{g/L}$  (Fig. 8).

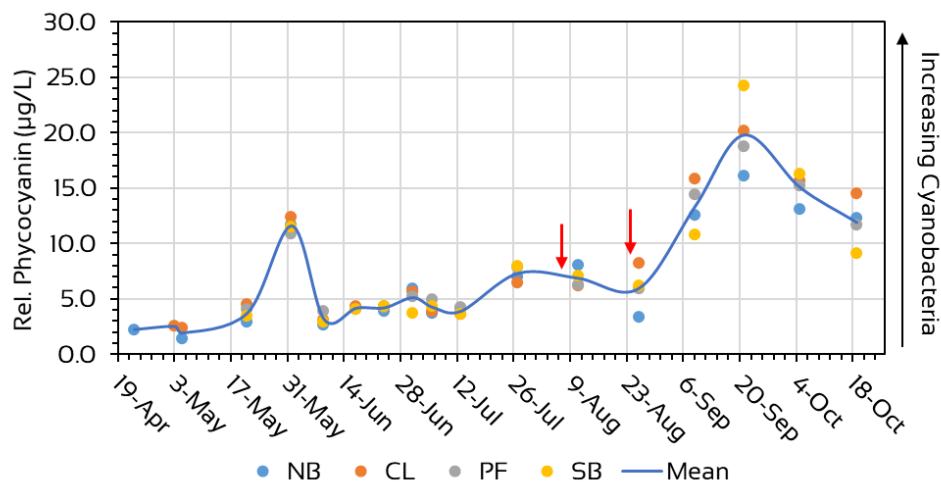


Figure 8. Average relative phycocyanin concentrations from measurements taken in the top three meters of the water column at the North Bay (NB), Center Lake (CL), Point Folly (PF), and South Bay (SB) sites during the 2020 season. The red arrows indicate the timing of the copper sulfate treatments that occurred on August 6th and August 24th.

From July 27<sup>th</sup> through August 26<sup>th</sup>, most site relative phycocyanin averages were between 5 and  $10\mu\text{g/L}$ . The one exception was the  $3.4\mu\text{g/L}$  average measured at the NB Site on August 26<sup>th</sup>. Averages at the other sites on that day were between 5.9 and  $8.3\mu\text{g/L}$ . Average relative concentrations rapidly increased between August 26<sup>th</sup> and September 21<sup>st</sup> when the lake average was  $19.8\mu\text{g/L}$  and individual site averages were between 16.1 and  $24.2\mu\text{g/L}$  (Fig. 8).

Average concentrations gradually decreased from September 21<sup>st</sup> through October 19<sup>th</sup> when the lake average was  $11.9\mu\text{g/L}$  and site averages were between 9.1 and  $14.5\mu\text{g/L}$ . It is worth noting that a surface bloom was also observed on October 19<sup>th</sup>. An effort was made to collect the relative phycocyanin concentration at the top few millimeters

of the water column at the NB and CL sites where relative concentrations were 18 and 30.7 $\mu\text{g/L}$ , respectively.

### Total Phosphorus Concentrations

Phosphorus in freshwater systems is most commonly the nutrient in shortest supply and in greatest demand by the algae; therefore, it often limits levels of algal productivity. Sources of phosphorus can be from external sources (e.g., from the watershed or atmosphere), or internal sources (e.g., released from bottom sediments under anoxic conditions). Total phosphorus represents all forms of phosphorus in a sample, i.e., particulate and soluble forms.

Average epilimnetic concentrations were 22.3 and 23.3 $\mu\text{g/L}$  at the NB and CL sites, respectively. Lowest concentrations at both sites occurred on July 13<sup>th</sup> and August 11<sup>th</sup>; and, were between 13 and 15 $\mu\text{g/L}$ . Highest epilimnetic concentrations at the NB site were on April 23<sup>rd</sup> and October 19<sup>th</sup> at 27 and 40 $\mu\text{g/L}$ , respectively. At CL, the April 23<sup>rd</sup> concentration was the highest at 30 $\mu\text{g/L}$  and was followed by the September 9<sup>th</sup> and October 19<sup>th</sup> concentrations of 28 and 27 $\mu\text{g/L}$ , respectively.

The metalimnetic average at NB of 22.7 $\mu\text{g/L}$  was nearly identical to the site's epilimnetic concentration. The seasonal trend was that the highest metalimnetic levels were at the beginning and end of the season. The metalimnetic average at CL of 43.9 $\mu\text{g/L}$  was higher than the site's epilimnetic level due – largely – to the September 9<sup>th</sup> concentration of 148 $\mu\text{g/L}$  (Fig. 9).

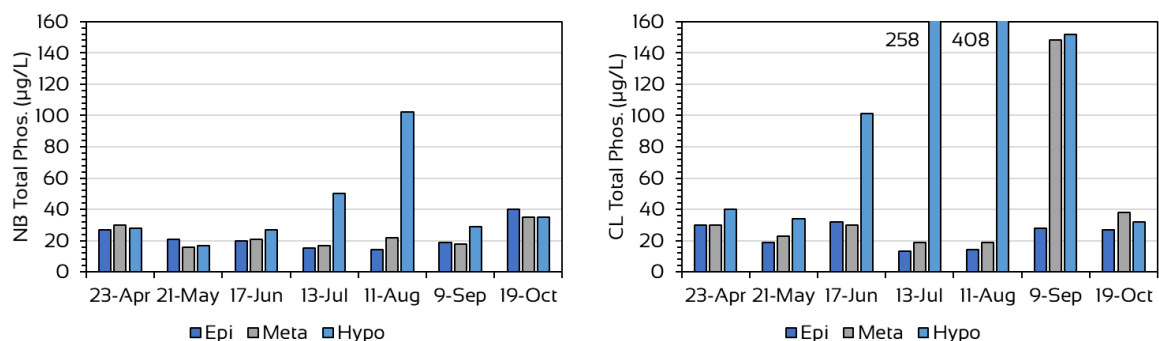


Figure 9. Total phosphorus (Phos.) concentrations in the epilimnion (Epi), metalimnion (Meta), and hypolimnion (Hypo) of the North Bay and Center Lake sites during the 2020 season.

Hypolimnetic total phosphorus concentrations did not differ notably from epilimnetic or metalimnetic concentrations early in the season at either site. At the CL site, the June 17<sup>th</sup> hypolimnetic concentration was three times greater than that at the other strata (Fig. 9). The hypolimnetic concentration at CL continued to increase through

August 11<sup>th</sup>, decreased marginally by September 9<sup>th</sup>, and further decreased to levels that were similar to those in the other strata by October 19<sup>th</sup>.

At the NB site, elevated hypolimnetic concentrations were not observed until July 13<sup>th</sup>. The hypolimnetic concentration continued to increase through August 11<sup>th</sup> before decreasing to epilimnetic and metalimnetic concentrations through September 9<sup>th</sup> to October 19<sup>th</sup>. It's worth noting that the maximum hypolimnetic concentration at NB, which was measured on August 11<sup>th</sup>, was observed nearly two months earlier at the CL site.

An ANOVA was performed comparing total phosphorus data from the three strata and from both sites. The only seasonal data that was significantly different ( $p < 0.05$ ) from the others was the hypolimnetic data from CL. Concentrations at the other strata from either site were not significantly different.

### *Nitrogen Concentrations*

Nitrogen is regularly the second most limiting nutrient for algae growth in freshwater systems. It can be present in a number of forms in lake water. Ammonia – a reduced form of nitrogen – is important because it can affect the productivity, diversity, and dynamics of the algal and plant communities. Ammonia can be indicative of internal nutrient loading since bacteria will utilize other forms of nitrogen (e.g., nitrite and nitrate) in lieu of oxygen for cellular respiration under anoxic conditions, resulting in ammonia enrichment of the hypolimnion.

Total Kjeldahl nitrogen (aka TKN) is a measure of the reduced forms of nitrogen (including ammonia) and total organic proteins in the water column. Since TKN accounts for biologically derived nitrogen-rich proteins in the water column, it is useful in assessing the productivity of the lentic system. Nitrate and nitrite are often below detectable levels in natural systems because they are quickly cycled by bacteria and aquatic plants. Total nitrogen is the sum total of TKN, nitrate, and nitrite. Since the latter two are often below detectable limits, TKN levels are often similar or equal to total nitrogen levels.

Nitrite was not detected in any of the samples collected in the epilimnion, metalimnion, or hypolimnion at either the NB or CL sites. Nitrate was detected only once when 59 µg/L were measured in the sample collected on September 9<sup>th</sup> in the hypolimnion of the NB site. Therefore, total nitrogen levels differed from TKN levels only in that one sample.

At the NB site, average TKN levels did not significantly differ ( $p > 0.05$ ); NB averages for the epilimnion, metalimnion, and hypolimnion were 448, 434, and 524 µg/L, respectively. Concentrations were generally between 300 and 500 µg/L with several notable exceptions, e.g., 690, 712, and 744 µg/L in the epilimnion, metalimnion, and hypolimnion, respectively, on October 19<sup>th</sup>; and, 846 µg/L in the hypolimnion on August 11<sup>th</sup>.

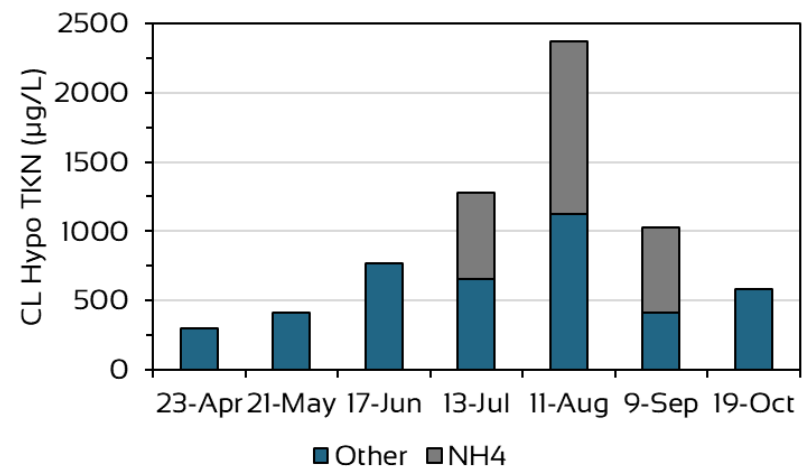
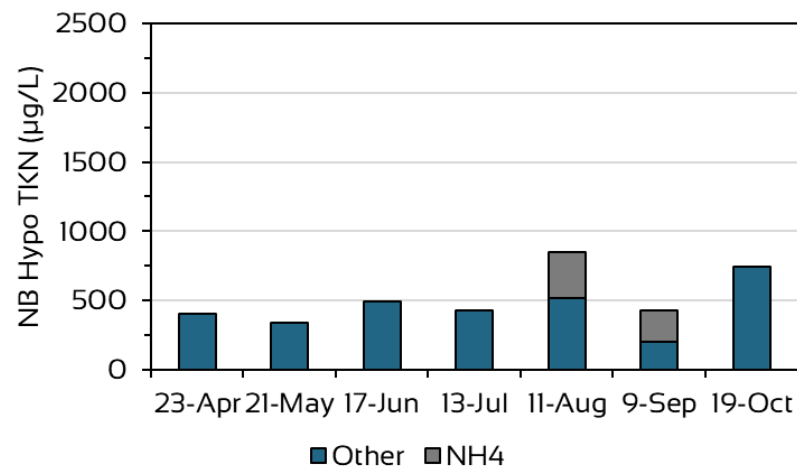
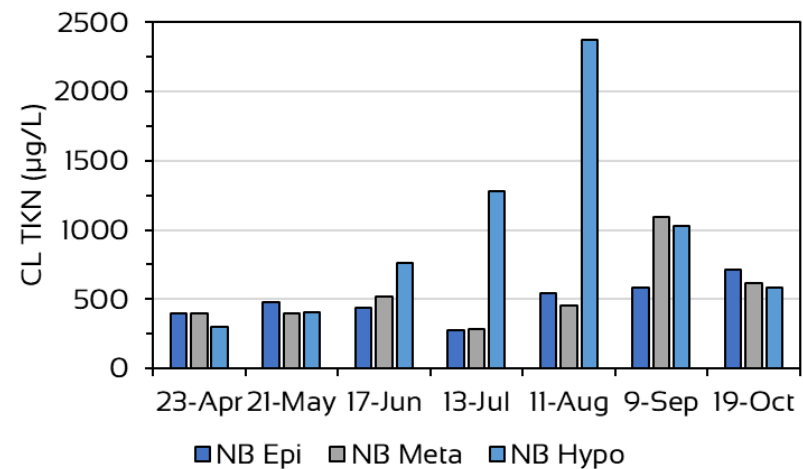
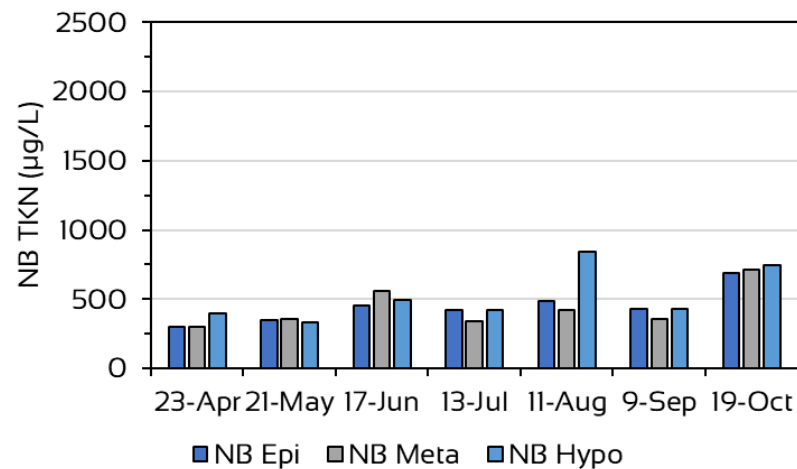


Figure 10. Top: Total Kjeldahl nitrogen (TKN) concentrations in the epilimnion (Epi), metalimnion (Meta), and hypolimnion (Hypo) at the North Bay (NB) and Center Lake (CL) sites in 2020. Bottom: TKN with the ammonia (NH<sub>4</sub>) component displayed in the hypolimnion of the NB and CL sites in 2020.

Season-average concentrations in the CL site epilimnion and metalimnion of 490 and 537µg/L, respectively, were higher than the NB counterparts but were not statistically different ( $p>0.05$ ). The CL concentrations at those strata gradually increased after the season lows on July 13<sup>th</sup> (Fig. 10). Concentrations in the metalimnion reached their maximum level of 1,090µg/L on September 9<sup>th</sup>; in the epilimnion concentrations reached their maximum of 713µg/L by October 19<sup>th</sup>.

The average concentration in the CL hypolimnion of 961µg/L was significantly higher ( $p<0.05$ ) than averages at all other strata of the CL or NB sites. CL hypolimnetic concentrations began to differentiate from concentrations in strata above (i.e., epilimnion and hypolimnion) by June 17<sup>th</sup> then increased to 2,370µg/L by August 11<sup>th</sup> then decreased to 579µg/L by October 19<sup>th</sup> (Fig. 10).

As noted earlier, TKN is a measure of reduced forms of nitrogen including ammonia. Ammonia was also measured separately in samples. An ammonia concentration of 118µg/L was detected in the NB epilimnetic sample collected on June 17<sup>th</sup> and constituted approximately 26% of the TKN. A higher concentration of 621µg/L was detected in the metalimnetic sample collected at the CL site on September 9<sup>th</sup> where it constituted 57% of TKN. The other five samples with measurable ammonia were from hypolimnetic samples collected between July 13<sup>th</sup> and September 9<sup>th</sup> (Fig. 10); and, constituted between 40 and 54% of TKN at the NB site and between 49 and 60% of TKN at the CL site during that timeframe.

## PELAGIC ALGAE COMMUNITY, CYANOBACTERIA, AND CYANOTOXINS

Qualitative and quantitative analyses of the algal community have been important components of lake water quality studies for many years. Algae as bioindicators can provide insight into levels of nutrients and other chemical characteristics of lake water. They are responsive to reductions and improvements to water quality. In recent years, analyses have focused on toxigenic algae in freshwaters.

Fifty-three different algal genera were identified in the phytoplankton net or whole water samples and were asymmetrically distributed among six taxonomic groups (Table 2). Two-thirds of those genera were from two taxonomic groups. The Chlorophyta (aka Green Algae) were represented by 24 different genera. The number of Cyanobacteria (aka Blue-green Algae) genera identified was 11. Bacillariophyta (aka Diatoms), Chrysophyta (aka Golden Algae), Pyrrophyta (aka Dinoflagellates), and Euglenophyta were collectively representative of 17 genera.

Cyanobacteria were the most dominant taxa for the entire season. They comprise 90% or more of the cell concentrations on 15 and 16 of the 19 dates the algal community was analyzed at the NB and CL sites, respectively. On all other dates, the Cyanobacteria comprised >80% of all cells with one exception. On September 4<sup>th</sup> at the NB



site, they comprised 65% of all cells with Chlorophyta, Chrysophyta, and Bacillariophyta each comprising between 10 and 12% of the cell concentration.

An important objective of the algae analyses was the provision of information that the BLPA could share with their stakeholders so informed decisions about the use of Bantam Lake for recreational purposes could be made. In the last several decades much has been learned about the toxicological nature of some Cyanobacteria genera and the threat to human and pet health when cell concentrations are high, e.g., in bloom conditions. The State of Connecticut now provides recommendations to municipal health departments about how to monitor conditions and what conditions/Cyanobacteria cell concentrations might pose threats (CT DPH & CT DEEP 2019).

The State recommends a visual assessment method to characterize conditions at public beaches supported by Cyanobacteria cell concentration analyses. Cyanobacteria cell concentrations of <20,000 cells/mL are considered characteristic of Visual Rank Category 1 and do not generally warrant any public mitigative measures. When cell concentrations are between 20,000 and 100,000 cells/mL, designated as Visual Rank Category 2, the State recommends posting Cyanobacteria warning signage, reporting the events to the State, and increasing vigilance. For concentrations >100,000, or Visual Rank Category 3, the State recommends the posting of beach closure signage.

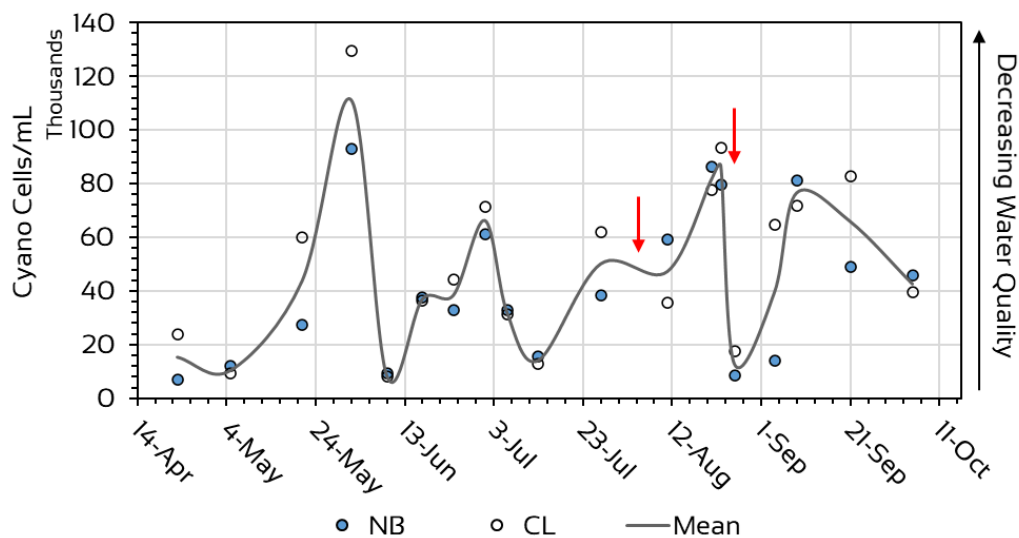


Figure 11. Cyanobacteria cell concentrations at the North Bay (NB) and Center Lake (CL) sites in 2020. The red arrows indicate the timing of the copper sulfate treatments that occurred on August 6th and August 24th.

Cyanobacteria cell concentrations at Bantam Lake were highly variable and spanned all three visual rank categories. Most of the concentrations fell within the Visual Rank Category 2 range (Fig. 11). Lower concentrations in April and May gave way to bloom conditions on June 1<sup>st</sup> with cell concentrations nearing or exceeding 100,000 cells/mL depending on site.

By June 9<sup>th</sup>, cell concentrations had markedly decreased. They increased again with much of June and July experiencing concentrations in the 30,000 to 71,000 cells/mL range. A copper sulfate treatment occurred on August 6<sup>th</sup> but the August 11<sup>th</sup> cell concentrations remained between 30,000 and 60,000 cells/mL. August 21<sup>st</sup> the 23<sup>rd</sup> concentrations increased to approximately 80,000 or more cells/mL before a second application of copper sulfate on August 24<sup>th</sup>. The second treatment appeared to have a greater efficacy; August 26<sup>th</sup> concentrations at the NB and CL sites decreased to the Visual Rank Category 1 range.

Concentrations remained low at the NB site on September 4<sup>th</sup> but increased to levels observed prior to the second treatment at the CL site (Fig. 11). By September 9<sup>th</sup>, concentrations at both sites were >70,000 cells/mL. Concentrations on September 21<sup>st</sup> remained high at the CL site on but decreased marginally at the NB site. By October 5<sup>th</sup>, the CL concentration decreased and was similar to the NB concentrations.

On the final water quality visit of the season on October 19<sup>th</sup> samples were collected from the top 5 cm of the water column, rather than integrating the top three meters of the water column, in order to understand concentrations at the surface during observable bloom conditions. Cyanobacteria cell concentrations were 404,663 and 637,751 cells/mL and well above the 100,000 cell/mL threshold when beach closure signage is recommended.

The algal community structure evolved over the course of the season. The dominant algal genus from early in the season through early July was the filamentous Cyanobacteria *Aphanizomenon* spp. (Fig. 12). Although not nearly as abundant as the Cyanobacteria, Chrysophyta and Bacillariophyta were an important component of the spring and early summer algal community. Genera such as *Dinobryon* spp., *Uroglenopsis* spp., and *Synura* spp. (Fig. 12) were commonly observed Golden Algae in samples collected during that time. Diatoms observed included *Asterionella* spp., *Aulocoseria* spp., and *Tabellaria* spp.

Diatoms maintained a presence for much of the season. Green Algae became a secondary component of the community as the Golden Algae became less important from mid to late summer. It was the mid-summer period when the filamentous Cyanobacteria *Dolichospermum* spp. (Fig. 12) replaced *Aphanizomenon* spp. as the dominant genus. *Aphanizomenon* spp. would often be observed as co-dominant with *Dolichospermum* spp. from late August through the end of the season.



Table 2. List of genera by taxonomic group identified in samples collected at Bantam Lake in 2020.

Chlorophyta	Cyanobacteria	Chrysophyta
<i>Anikistrodesmus sp.</i>	<i>Aphanizomenon sp.*</i>	<i>Dinobryon sp.</i>
<i>Arthrodesmus sp.</i>	<i>Aphanocapsa sp.*</i>	<i>Mallomonas sp.</i>
<i>Coelastrum sp.</i>	<i>Aphanothece sp.*</i>	<i>Synura sp.</i>
<i>Crucigenia sp.</i>	<i>Chroococcus sp.*</i>	<i>Uroglenopsis sp.</i>
<i>Dictyosphaerium sp.</i>	<i>Coelosphaerium sp.</i>	
<i>Elakatothrix sp.</i>	<i>Dolichospermum sp.*</i>	
<i>Eudorina sp.</i>	<i>Microcystis sp.*</i>	<b>Pyrrhophyta</b>
<i>Golenkinia sp.</i>	<i>Oscillatoria sp.*</i>	<i>Ceratium sp.</i>
<i>Gloeocystis sp.</i>	<i>Pseudoanabaena sp.*</i>	<i>Glenodinium sp.</i>
<i>Gonium sp.</i>	<i>Snowella sp.*</i>	<i>Gymnodinium sp.</i>
<i>Micractinium sp.</i>	<i>Woronichinia sp.*</i>	<i>Peridinium sp.</i>
<i>Mougeotia sp.</i>		
<i>Nephrocytium sp.</i>		
<i>Oocystis sp.</i>	<b>Bacillariophyta</b>	<b>Cryptophyta</b>
<i>Padorina sp.</i>	<i>Asterionella sp.</i>	<i>Cryptomonas ovata</i>
<i>Pediastrum sp.</i>	<i>Aulocoseria sp.</i>	
<i>Quadrigula sp.</i>	<i>Fragilaria sp.</i>	
<i>Scenedesmus sp.</i>	<i>Stephanodiscus sp.</i>	<b>Euglenophyta</b>
<i>Schroederia sp.</i>	<i>Synedra sp.</i>	<i>Euglena sp.</i>
<i>Selenastrum sp.</i>	<i>Tabellaria sp.</i>	<i>Trachelomonas sp.</i>
<i>Staurastrum sp.</i>		
<i>Tetraedron sp.</i>		
<i>Ulothrix sp.</i>		

\* Indicates a Cyanobacteria genera that is considered toxigenic.

### Relative Phycocyanin Profiles

Certain Cyanobacteria, including several of those observed at Bantam Lake (e.g., *Aphanizomenon spp.*, *Dolichospermum spp.*, and *Microcystis spp.*), have the ability to regulate their buoyancy. Visible blooms are the result of many Cyanobacteria cells becoming so positively buoyant that they reach the surface. Cyanobacteria can be observed unequally distributed or layered at specific depths in water column. To assess vertical and temporal distribution, the photosynthetic pigment unique to the Cyanobacteria was measured during visits throughout the water column with the fluorimeter incorporated into the sensor array of the Eureka Manta II multiprobe. Fluorimeters work on the principal that a particular substance fluoresces at a specific wavelength

when light of another wavelength is directed on that substance. The fluorimeter in AER's field instrumentation emits a wavelength that interacts with phycocyanin. This sensor is not calibrated to known concentrations of phycocyanin so measurements are not quantitative; instead the measurements are relative to other measurements in the water column or to other sites.

Relative phycocyanin isopleths aligned with other data identifying the bloom conditions observed in early June and later in the season. The June 1<sup>st</sup> bloom was limited to depths above the thermocline at the NB, CL, and FP sites but encompassed the entire water column at the SB site (Fig. 13). Highest concentrations of phycocyanin were observed near or below the thermocline in late July through early August at the NB, CL, and FP sites. During the bloom conditions in September, phycocyanin concentrations were high throughout the water column at all sites with highest concentrations observed on September 21<sup>st</sup>.

### *Microcystin Monitoring*

Last year, the BLPA engaged Dr. Edwin Wong in the Biology and Environmental Science Department at Western Connecticut State University to measure microcystin levels in samples in waters collected by AER from the top three meters of the water column during biweekly visits. Microcystin is one of the most common of a number of cyanotoxins produced by Cyanobacteria. The State of Connecticut recommends using a threshold of 8µg/L, above which beach closure signage should remain deployed. These analyses were continued in 2020 with data presented in Table 3. Despite high concentrations of Cyanobacteria cells and phycocyanin, microcystin levels never exceeded 1µg/L and only exceeded 0.5µg/L once which was measured in the sample collected on July 27<sup>th</sup> from the CL site.

Table 3. Microcystin concentrations in µg/L in samples collected at Bantam Lake in 2020.

DATE	CENTER LAKE	NORTH BAY
5/21/2020	0.05	0.041
6/1/2020	0.061	0.282
6/17/2020	0.124	0.336
7/1/2020	0.116	0
7/13/2020	0.049	0.053
7/27/2020	0.237	0.755
8/10/2020	0.133	0.19
8/27/2020	0.167	0.253
9/9/2020	0.131	0.194
9/21/2020	0.313	0.168
10/5/2020	0.238	0.234
10/23/2020	0.153	0.195

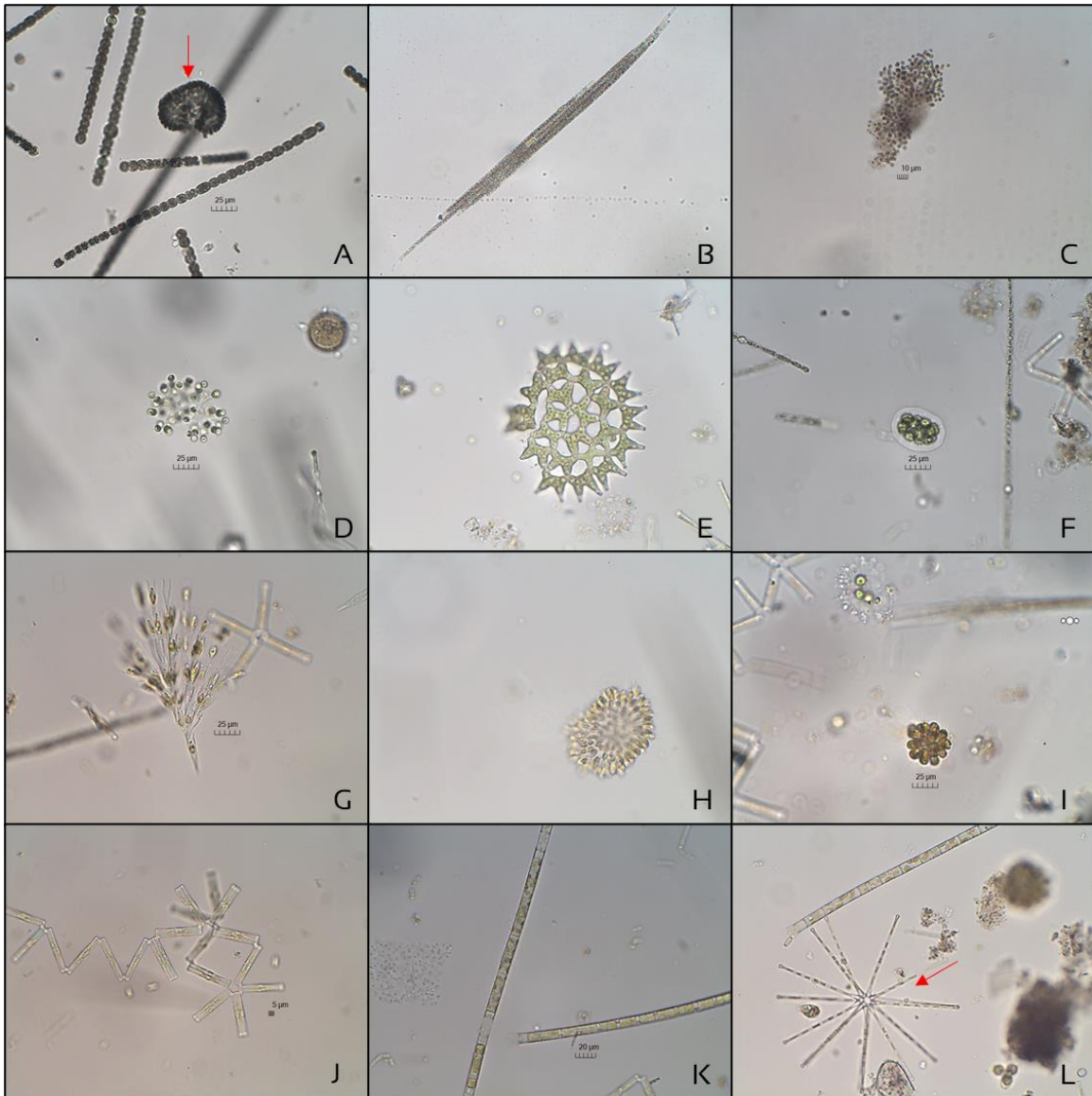


Figure 12. Micrographs of specimens of algae genera collected from Bantam Lake in 2020. Cyanobacteria (aka Blue-Green Algae) genera included A) *Dolichospermum* sp. and *Coelosphaerium* sp. (red arrow), B) *Aphanizomenon* sp., and C) *Microcystis* sp.; Chlorophyta (aka Green Algae) D) *Dictyosphaerium* sp., E) *Pediastrum* sp., and F) *Padorina* sp.; Chrysophyta (aka Golden Algae) G) *Dinobryon* sp., H) *Uroglenopsis* sp., and I) *Synura* sp.; Bacillariophyta (aka Diatoms) J) *Tabellaria* sp., K) *Aulocoseria* sp., and L) *Asterionella* sp. (red arrow). Total magnification for all micrographs = 400X.

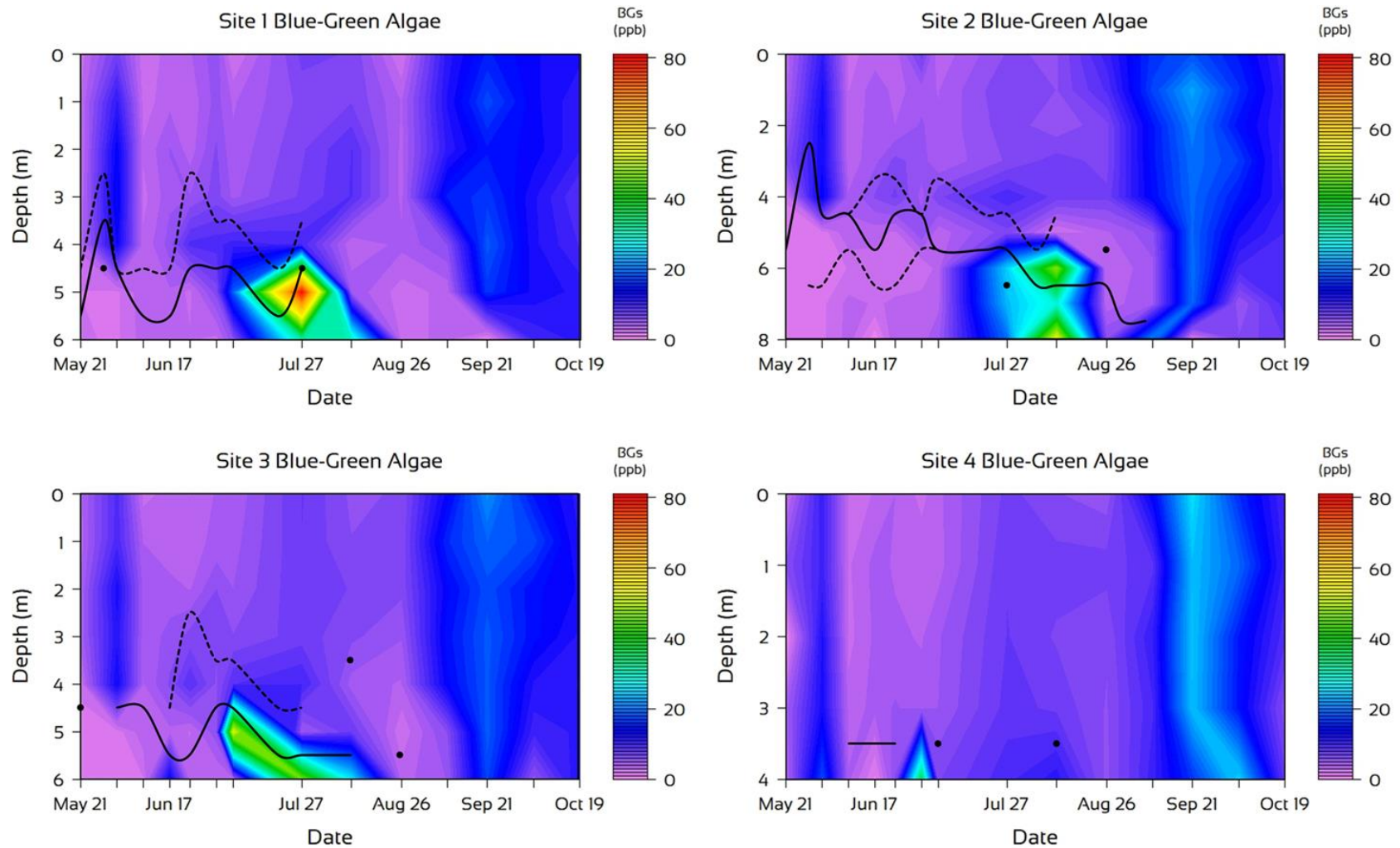


Figure 13. Isopleths of relative phycocyanin concentrations at the North Bay (Site 1), Center Lake (Site 2), Folly Point (Site 3), and South Bay sites in 2020. The dashed lines represent the upper or lower boundary of the metalimnion and the solid lines or points represents the thermocline.

## CHEMICAL ASSESSMENT

### *Specific Conductance*

Conductivity is a surrogate measurement of the dissolved salt or ion concentration in water; as the name suggests, it is a measure of water's ability to conduct an electrical current. Data collection begins with a measure of conductivity. That datum is converted to specific conductance by mathematically standardizing it to a set water temperature (25°C) because – in the field – temperature varies with depth and/or date and alters the ability of water to conduct an electrical current.

Specific conductance is an important metric in Limnological studies due to its ability to detect pollutants and/or nutrient loadings. Specific conductance can also have an influence on organisms that inhabit a lake or pond; particularly, algae. The composition of algal communities has been shown to be related, in part, to conductivity levels in lakes (e.g., Siver 1993, McMaster & Schindler 2005).

Specific conductance near the lake bottom sediments can be higher than in shallower depths of the water column nearer to the surface; particularly, later in the summer after the water column has been stratified and the waters near bottom have been anoxic for protracted periods of time. Under those conditions, minerals and salts in the sediments can undergo chemical transformation and change from a particulate state to a dissolved ionic state, diffuse to the waters above the sediments, and increase the conductivity of the hypolimnion.

Specific conductance data collected throughout the water column over the 2020 season were utilized in the development of isopleth diagrams for each site (Fig. 14). From those, differences in specific conductance were observed over time and depth within the water columns. Early season specific conductance through May 21<sup>st</sup> was lowest, with values between 165 and 175  $\mu\text{S}/\text{cm}$ , and fairly uniform throughout the water column.

After May 21<sup>st</sup> and through October 19<sup>th</sup>, specific conductance gradually increased above the thermocline with levels of 190 to 195  $\mu\text{S}/\text{cm}$  commonly observed after July 27<sup>th</sup> (Fig. 14). The elevated levels above the thermocline persisted through to the last sight visits on October 19<sup>th</sup>.

Specific conductance below the thermocline exhibited much more dynamic change, particularly between mid-June and toward the end of September (Fig. 14). The most dynamic changes occurred at the CL site where specific conductance of >210  $\mu\text{S}/\text{cm}$  were common from 6m of depth to the bottom. Measurements of 314 and 311  $\mu\text{S}/\text{cm}$  were recorded on June 17<sup>th</sup> and August 26<sup>th</sup>, respectively at the bottom (8m of depth). The period of July 27<sup>th</sup> to August 26<sup>th</sup> exhibited the greatest specific conductance levels below the thermocline at the CL site, when readings of 220 to 240  $\mu\text{S}/\text{cm}$  were recorded at 6m; 260 to 285  $\mu\text{S}/\text{cm}$  recorded at 7m; and 264 to 311  $\mu\text{S}/\text{cm}$  recorded at 8m of depth. Levels afterwards decreased to epilimnetic levels by October 19<sup>th</sup> (Fig. 14).



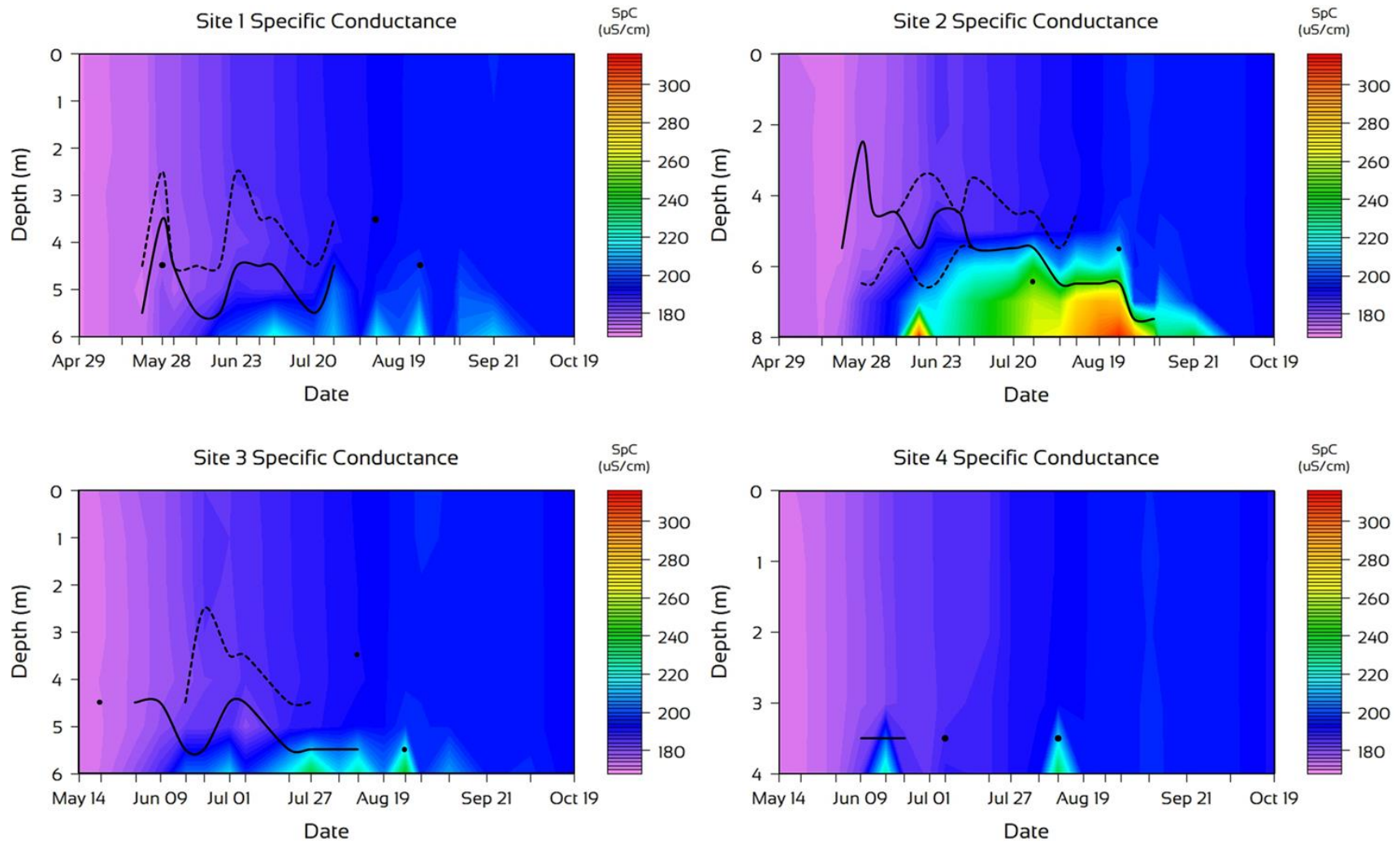


Figure 14. Isopleths of specific conductance (SpC) at the North Bay (Site 1), Center Lake (Site 2), Folly Point (Site 3), and South Bay sites in 2020. The dashed lines represent the upper or lower boundary of the metalimnion and the solid lines or points represents the thermocline.

Elevated specific conductance below the thermocline at the NB, FP, and SB sites were observed intermittently in the July 27<sup>th</sup> to August 26<sup>th</sup> timeframe, were generally relegated to the very bottom of the water column, and never reached the levels observed at the CL site. The FP site – the site nearest to the CL site – was most similar with measurements of 228 to 242  $\mu\text{S}/\text{cm}$  at 6m of depth during that period of time. A maximum specific conductance of 221  $\mu\text{S}/\text{cm}$  was observed on August 26<sup>th</sup> at the NB site; and a maximum at the SB site of 236  $\mu\text{S}/\text{cm}$  was recorded on August 8<sup>th</sup>.

To examine differences between sites and depth, an Analysis of Variance (ANOVA) was performed using the measurements at all depths for each site, and at all depths and all sites (Fig. 15). Significant differences of specific conductance averages were only observed among depths of the CL site ( $p < 0.05$ ). Differences in averages at each depth of the other sites were not significant ( $p > 0.05$ ).

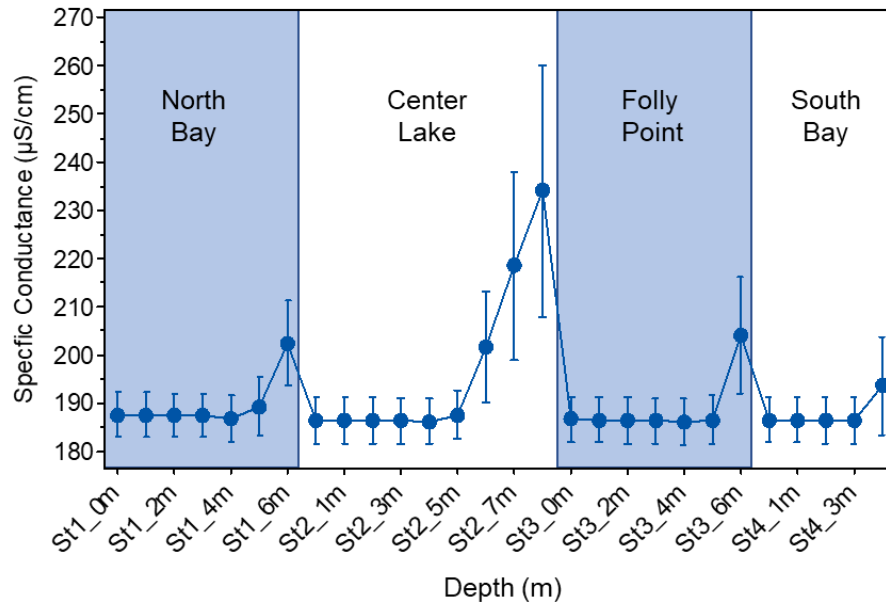


Figure 15. Results of ANOVA using specific conductance measurements at each depth during the 2020 season. Error bars represent on standard deviation.

Significant differences were also established using all depths at all sites ( $p < 0.005$ ) and due to the elevated averages at the CL site. It is worth noting that averages and standard deviations at the 6m strata of NB, CL, and FP sites were similar.



## Iron and Manganese

Soluble iron and manganese concentrations in lake waters provide useful insights into the dynamics of the internal loading of phosphorus from anoxic lake sediments. In New England, oxidized iron compounds sequester phosphorus in lake sediments making it unavailable to the algae community in a particulated form. After depletion of oxygen in the surface sediments via aerobic cellular respiration, and provided that oxygen concentrations are not replenished, the microbial metabolic processes and composition of the microbes carrying out those processes shift.

After oxygen is no longer available, other oxidizing agents are used sequentially in anaerobic respiration including nitrate, manganese, and iron. Once the iron compounds binding the phosphates are used, the iron and orthophosphates become soluble, diffuse, and accumulate in waters overlying the sediments. Although oxidized manganese compounds do not sequester phosphorus, they are the compounds used just before iron in the series of anaerobic oxidizing agent. Iron concentrations in the epilimnion were undetectable to very low ( $\leq 0.11\text{mg/L}$ ) at both the NB and CL sites. The epilimnetic season average was  $0.05\text{mg/L}$  at both sites.

Hypolimnetic iron season averages were  $0.53$  and  $3.93\text{mg/L}$  at the NB and CL sites, respectively. The hypolimnetic CL average was significantly greater than the hypolimnetic NB average, and both epilimnetic averages ( $p < 0.005$ ). The NB hypolimnetic average was not significantly higher than epilimnetic averages ( $p > 0.05$ ).

Concentrations on April 23<sup>rd</sup> were undetectable at both the top and bottom of the water column. On May 21<sup>st</sup>, very low concentrations were detected. Concentrations remained low in both strata of the NB site on June 17<sup>th</sup>; at the CL site, the hypolimnetic concentration experienced a 27-fold increase (Fig. 16).

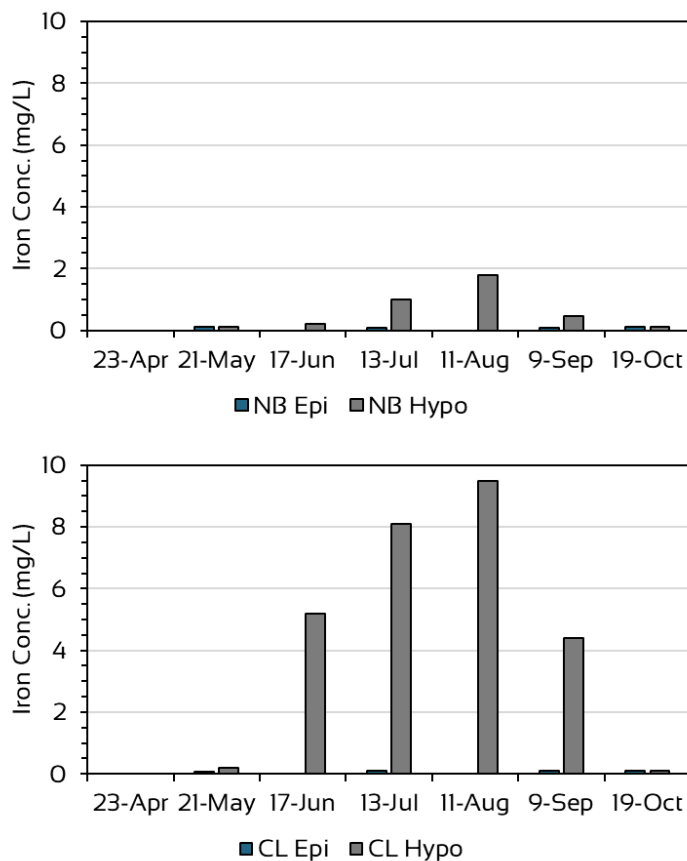


Figure 16. Concentrations of iron in the epilimnion (Epi) and hypolimnion (Hypo) of the North Bay (NB; top) and Center Lake (CL; bottom) sites in 2020.

Concentration in the hypolimnion of the CL site continued to increase through August 11<sup>th</sup> when it reached a maximum of 9.5mg/L. At the NB site, a more subtle increase was observed through August 11<sup>th</sup> (Fig. 16). Hypolimnetic concentrations decreased at both sites by September 9<sup>th</sup>, but were still relatively high at the CL site. By October 19<sup>th</sup>, hypolimnetic concentrations were low and similar to epilimnetic concentrations at both sites.

Analyses of soluble manganese in the epilimnion and hypolimnion of the NB and CL sites produced results similar to those from iron analyses. The average epilimnetic concentration of 0.03mg/L at both sites, and the hypolimnetic average at the NB site of 0.41mg/L were all significantly lower than the CL hypolimnetic concentration of 1.35mg/L ( $p < 0.05$ ).

The greatest increase in hypolimnetic levels occurred between May 21<sup>st</sup> and June 17<sup>th</sup>, while the greatest increase in the NB hypolimnion occurred between June 17<sup>th</sup> and July 13<sup>th</sup> (Fig. 17). Hypolimnetic concentrations reached their maximum levels on August 11<sup>th</sup> before decreasing to epilimnetic levels by October 19<sup>th</sup>.

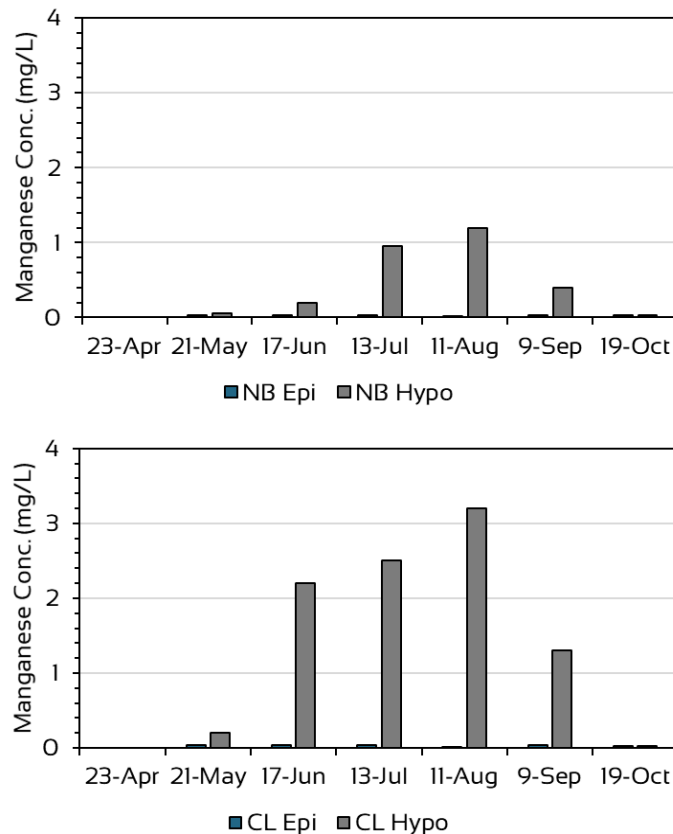


Figure 17. Concentrations of manganese in the epilimnion (Epi) and hypolimnion (Hypo) of the North Bay (NB) and Center Lake (CL) sites in 2020.

### Alkalinity and pH

Alkalinity is a measure of calcium carbonate, and reflects the acid neutralizing capacity of water (i.e., buffering capacity). Alkalinity of surface waters is largely influenced by local geology and other watershed characteristics. Alkalinity at the bottom of the water column can also be generated internally from the biologically mediated reduction of iron, manganese, and sulfate via cellular respiration in the anoxic lake sediments, and denitrification of nitrate to elemental nitrogen (Wetzel 2001).

At the NB site, average epilimnetic, metalimnetic and hypolimnetic alkalinities were 40.3, 40.6, and 41.7mg/L. Averages were not significantly different from each other ( $p>0.05$ ). A gradual increase at all strata was observed between April 23<sup>rd</sup> and September 9<sup>th</sup>. Levels throughout the water column early in the season of 34 and 36mg/L increased to 45 to 55mg/L by September 9<sup>th</sup> (Fig. 18). Alkalinity decreased some by October 19<sup>th</sup>.

A similar pattern was observed in the epilimnion and metalimnion of the CL site. Alkalinity in the hypolimnion diverged from that observed at the NB site (Fig. 18). From May 21<sup>st</sup> through August 11<sup>th</sup>, hypolimnetic alkalinity at the CL site steadily increased from 36 to 80mg/L before decreasing to 42mg/L by October 19<sup>th</sup>.

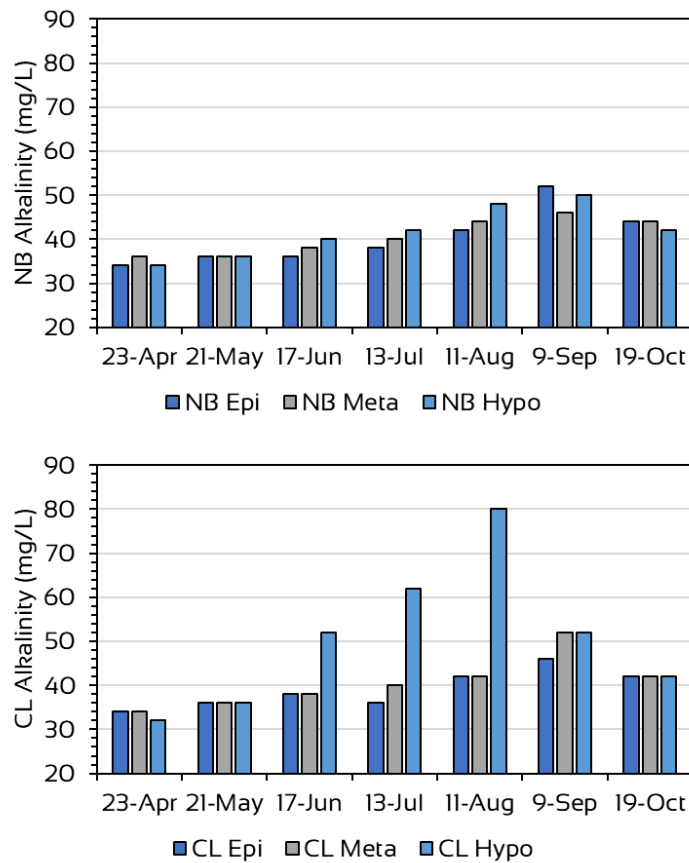


Figure 18. Alkalinity in the epilimnion (Epi), metalimnion (Meta), and hypolimnion (Hypo) of the North Bay (NB) and Center Lake (CL) sites in 2020.

The pH of lake water is important for several reasons. Firstly, very low or very high pH levels will not support diverse lentic fauna and flora. Algal communities are influenced by pH due – in part – to the forms of dissolved carbon in the water column. For example, at pH greater than 8.3, bicarbonate is the dominant form of carbon available to the pelagic algal community; the blue-green algae have adaptive advantages over other algal groups under those conditions because they are able to efficiently utilize that form of carbon. Other algal groups are dependent upon carbon dioxide, which becomes limited in water above pH of 8.3.

The lake wide, epilimnetic pH average, minimum and maximum levels were 8.3, 7.8 and 9.0, respectively. Epilimnetic averages among all sites were not significantly different ( $p>0.05$ ). Average epilimnetic pH levels were significantly higher than hypolimnetic averages ( $p<0.05$ ). Among the hypolimnetic pH averages, the SB site average was significantly higher than the average of the other three sites. The average hypolimnetic

pH for NB, CL, FP, and SB were 7.3, 7.4, 7.3, and 7.8, respectively. The mid-season hypolimnetic levels at all sites tended to be more similar across sites, while early and late season levels were more disparate (Fig. 19).

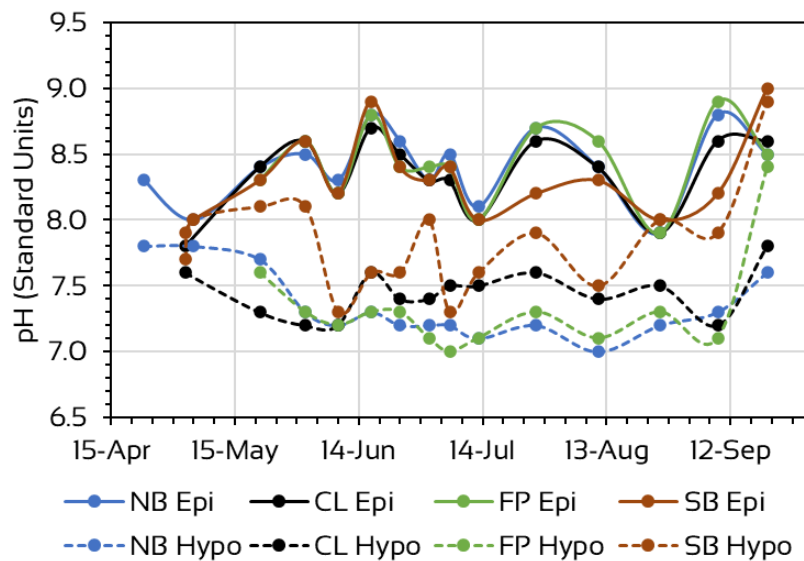


Figure 19. pH levels in the epilimnion (Epi) and hypolimnion (Hypo) at the North Bay (NB), Center Lake (CL), Folly Point (FP), and South Bay (SB) sites in 2020.

The difference between the epilimnetic and hypolimnetic pH levels was likely due to higher concentration of carbon dioxide ( $\text{CO}_2$ ) near the bottom. Carbon dioxide in water creates carbonic acid which is a weak acid but one that will lower pH. The small amount of  $\text{CO}_2$  in the atmosphere (0.04%) does diffuse into the water and is utilized by photosynthesizing organisms (e.g., plants and algae). Carbon dioxide is also generated by cellular respiration, which occurs throughout the water column. Photosynthesis decreases with depth due to lack of light energy resulting in increasing  $\text{CO}_2$  concentrations.

At the SB site, the relatively shallow water column (approximate 4m) was mixed through June 1<sup>st</sup>, exhibited periods of stratification and mixing through August 11<sup>th</sup>, and was consistently mixed afterwards. The more frequent mixing at the SB site explains why its hypolimnetic pH was more similar to epilimnetic pH as compared to hypolimnetic pH at the other sites.

### Base Cations and Chloride

Base cation and anion concentrations are important in understanding natural influences (e.g., dissolved salts from bedrock geology) as well as anthropogenic influences

in the watershed (e.g., road salts). In most lakes, the dominant base cations in lake waters are calcium ( $\text{Ca}^{2+}$ ), magnesium ( $\text{Mg}^{2+}$ ), sodium ( $\text{Na}^+$ ) and potassium ( $\text{K}^+$ ). Dominant anions include chloride ( $\text{Cl}^-$ ), sulfate ( $\text{SO}_4^{2-}$ ), and the alkalinity ions – carbonate ( $\text{CO}_3^{2-}$ ), and bicarbonate ( $\text{HCO}_3^-$ ). Those cations and anions are what collectively contribute to conductivity levels in lake water. The ratios of those ions and combinations of those ions can be diagnostic when compared to other lakes, and when compared to levels in the same lake over time.

We reported monthly base cations, chloride, and the alkalinity anion data by their mass (mg/L) and by their electrochemical equivalents (meq/L). The latter is performed by dividing the measured mass of an ion by its equivalent weight, which accounts for the ionic charge (positive or negative).

On a mass basis (mg/L), alkalinity comprised a majority of the ions measured, followed by chloride. On an electrochemical basis (meq/L), those two anions contributed equally. Since lake water is charged balance (collective amounts of positively charged cations equals the collective amounts of negatively charged anions in meq/L), the sum total of sodium, potassium, calcium, and magnesium were approximately equal to the total of anions. At the NB site, the average base cations and average anions measured here were 1.79 and 1.64 meq/L, respectively. At the CL site, concentrations were 1.65 and 1.60 meq/L, respectively. The difference was likely due to the anion, sulfate, not measured here.

Of the base cations, sodium and calcium were similar in their contribution to ionic concentrations, while magnesium contributed less (Fig. 20, Table 4). Potassium was a minor contributor to ion levels.

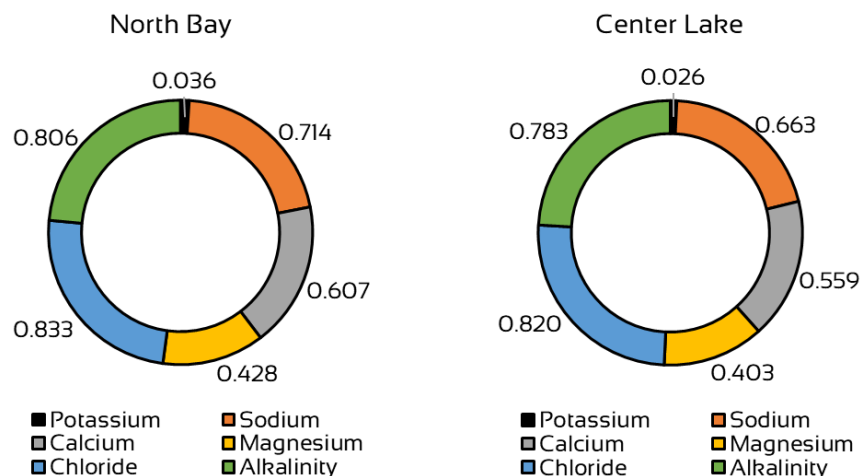


Figure 20. Average base cation, chloride and alkalinity ion concentrations at the North Bay (left) and Center Lake (right) sites in meq/L during the 2020 season.

Table 4. Base cations potassium (K<sup>+</sup>), sodium (Na<sup>+</sup>), calcium (Ca<sup>2+</sup>), magnesium (Mg<sup>2+</sup>), chloride (Cl<sup>-</sup>), and alkalinity ions (Alk) at the North Bay (NB) and Center Lake (CL) sites in 2020 in both mg/L and meq/L. ND = not detectable. Average (Avg) and standard deviation (STDEV) are calculated.

		K <sup>+</sup>		Na <sup>+</sup>		Ca <sup>2+</sup>		Mg <sup>2+</sup>		Cl <sup>-</sup>		Alk	
Site	Date	Mg /L	Meq /L	Mg /L	Meq /L	Mg /L	Meq /L	Mg /L	Meq /L	Mg /L	Meq /L	Mg /L	Meq /L
NB	23-Apr	1.4	0.04	15	0.65	11	0.55	4.7	0.39	27	0.77	34	0.68
NB	21-May	ND	ND	16	0.70	12	0.60	ND	ND	27	0.77	36	0.72
NB	17-Jun	ND	ND	19	0.83	13	0.65	5.5	0.46	30	0.86	36	0.72
NB	13-Jul	ND	ND	16	0.70	11	0.55	4.8	0.40	28	0.80	38	0.76
NB	11-Aug	ND	ND	16	0.70	12	0.60	5.1	0.43	32	0.91	42	0.84
NB	9-Sep	ND	ND	17	0.74	13	0.65	5.6	0.47	28	0.80	52	1.04
NB	19-Oct	ND	ND	16	0.70	13	0.65	5.5	0.46	29	0.83	44	0.88
NB	Avg	1.4	0.04	16.4	0.71	12.1	0.61	5.2	0.43	28.71	0.82	40.3	0.81
NB	ST DEV	---	---	1.3	0.06	0.90	0.04	0.39	0.03	1.80	0.05	6.3	0.13

		K <sup>+</sup>		Na <sup>+</sup>		Ca <sup>2+</sup>		Mg <sup>2+</sup>		Cl <sup>-</sup>		Alk	
Site	Date	mg/L	meq/L	mg/L	meq/L	mg/L	meq/L	mg/L	meq/L	mg/L	meq/L	mg/L	meq/L
CL	23-Apr	1	0.03	9.8	0.43	7.3	0.37	3.2	0.27	28	0.80	34	0.68
CL	21-May	ND	ND	15	0.65	11	0.55	ND	ND	27	0.77	36	0.72
CL	17-Jun	ND	ND	19	0.83	12	0.60	5.4	0.45	28	0.80	38	0.76
CL	13-Jul	ND	ND	16	0.70	11	0.55	4.8	0.40	27	0.77	36	0.72
CL	11-Aug	ND	ND	16	0.70	12	0.60	5	0.42	32	0.91	42	0.84
CL	9-Sep	ND	ND	16	0.70	13	0.65	5.7	0.48	28	0.80	46	0.92
CL	19-Oct	ND	ND	15	0.65	12	0.60	5.3	0.44	28	0.80	42	0.84
CL	Avg	1.0	0.03	15.3	0.66	11.2	0.56	4.9	0.41	28.3	0.81	39.1	0.78
CL	ST DEV	---	---	2.8	0.12	1.85	0.09	0.89	0.07	1.7	0.05	4.3	0.09



## MAJOR FINDINGS

### *Trophic Status*

A lake's trophic state or status is an account of the level of productivity, particularly open water algal productivity, that a lake supports. Average summer chlorophyll-*a* concentration and Secchi disk transparency provide direct measures of productivity and are used in conjunction with the average levels of nutrients that can limit algal productivity (i.e., total phosphorus and total nitrogen). Table 5 provides a standard framework of how those variables are used to assess trophic status developed in Connecticut.

Table 5 . Trophic classification criteria used by the Connecticut Experimental Agricultural Station (Frink and Norvell 1984) and the CT DEP (1991) to assess the trophic status of Connecticut lakes. The categories range from oligotrophic or least productive to highly eutrophic or most productive.

Trophic Category	Total Phosphorus ( $\mu\text{g} / \text{L}$ )	Total Nitrogen ( $\mu\text{g} / \text{L}$ )	Summer Chlorophyll- <i>a</i> ( $\mu\text{g} / \text{L}$ )	Summer Secchi Disk Transparency (m)
Oligotrophic	0 - 10	0 - 200	0 - 2	>6
Early Mesotrophic	10 - 15	200 - 300	2 - 5	4 - 6
Mesotrophic	15 - 25	300 - 500	5 - 10	3 - 4
Late Mesotrophic	25 - 30	500 - 600	10 - 15	2 - 3
Eutrophic	30 - 50	600 - 1000	15 - 30	1 - 2
Highly Eutrophic	> 50	> 1000	> 30	0 - 1

Bantam Lake average Secchi disk transparency in 2020 was 2.11m. The average transparency based on measurements taken from June through September was 2.06m. In both instances, average Secchi disk transparency was within the late mesotrophic range. It is worth noting that of the 92 Secchi disk transparency measurements, 42 of those were <2m, one was <1m (Fig. 6), and the season average for the SB site was <2m. These are reflective of eutrophic or even highly eutrophic conditions (Table 5).

Average chlorophyll-*a* concentration was 8.5 $\mu\text{g}/\text{L}$  and characteristic of mesotrophic productivity. Similar to Secchi transparency, average chlorophyll-*a* based on measurements from June through September (7.9 $\mu\text{g}/\text{L}$ ) did not reflect a different trophic classification. These data were representative of samples that were integrations of the top





Figure 21. Photographs of the Cyanobacteria surface scum at Bantam Lake taken on September 21, 2020.

three meters of the water column. During bloom conditions, much of the Cyanobacteria formed visible scums on the surface due to their ability to regulate their buoyancy (Fig 21). Therefore, the integrated samples may have underestimated Cyanobacteria biovolume if much of it was at the surface.

The average epilimnetic total phosphorus concentrations at the NB and CL sites in 2020 were 22.3 and 23.3  $\mu\text{g/L}$ , respectively and characteristic of mesotrophic productivity. Average concentrations in the hypolimnion were 41.1 and 146.4  $\mu\text{g/L}$  at the respective sites, which could support productivity commensurate with eutrophic and highly eutrophic conditions. Measured hypolimnetic concentrations diverged from epilimnetic concentrations by June 17<sup>th</sup> at the CL site, and by July 13<sup>th</sup> (Fig. 9).

#### *Internal Loading and Cyanobacteria Dynamics*

Elevated total phosphorus concentrations in the lower strata were observed both when the water columns were stratified and when they were not. When stratified and for much of July, highest concentrations of relative phycocyanin (i.e., Cyanobacteria) were at or below the thermocline which also comprised the lower boundary of the metalimnion (Fig. 13). In some instances, phosphorus concentrations at the lower depths of the water column remained elevated when a thermocline was not detected (e.g., September 9<sup>th</sup> at the CL site). Elevated relative phycocyanin concentrations appeared more equally distributed throughout the water column after destratification (Fig. 13).

The scenario described above implies that the Cyanobacteria were regulating buoyancy to take advantage of the higher phosphorus and other nutrient concentrations at lower depths when the lake was stratified in July. It is worth noting that at the CL site, anoxic and presumably phosphorus enriched waters, were observed above the thermocline after August 11<sup>th</sup> (Fig. 3). By the next sampling date of September 9<sup>th</sup>, the total

phosphorus concentrations in the CL mid-depth sample (designated metalimnion) were as high as the concentrations near the bottom of the water column (Fig. 9).

The elevated concentrations of phosphorus at the lower strata of the water column were driven by internal loading and this phenomenon, which annually occurs at Bantam Lake, is corroborated by much of the data collected in the monitoring program. Those data include:

1. Elevated concentrations of total phosphorus at the lower depths (Fig. 9)
2. Anoxic conditions and ORP of <200mV at the lower strata (Figs. 3, 4, 5)
3. Elevated ammonia, manganese, and ferrous iron at the lower depths (Figs. 10, 16, 17) – These are indicators of an environment where other oxidizing agents in anoxic lake sediments are used in cellular respiration after oxygen is depleted. Nitrates are first used resulting in loading of ammonia; then manganese. When the ferric iron is used and reduced, it and the phosphorus bound to it undergo a chemical transformation, becoming soluble, and load into overlying waters.
4. Dissimilatory reduction of compounds such as nitrate and sulfate during anaerobic cellular respiration result in the generation of alkalinity, which also increased at the lower depths of the Bantam water column, particularly at the CL site where stratification persisted longer (Fig. 18).
5. Elevated specific conductance at the lower depths (Fig. 14) – This is particularly evidenced at the CL site – as minerals transform into their dissolved state under anoxic conditions.

For the last three years, we have performed basic assessments of the average mass of phosphorus in Bantam Lake using the estimated volumes of water at each depth of the lake, assessment of stratification using temperature profile data at the NB and CL sites, and concentrations of phosphorus at the three strata of the water column where samples were collected at the NB and CL sites.

One shortcoming of these analyses is the assumption that the concentration at one strata of a particular layer (e.g., epilimnion or hypolimnion) represents the concentration throughout that layer, e.g., a concentration measured 0.5m above the bottom is representative of the concentration of all strata within the hypolimnion. Although a better understanding of the distribution of phosphorus concentrations throughout the water column (i.e., sampling and measuring concentrations at more depths) might be preferred, our analyses does provide important insights.

Much of the phosphorus in the lake resides in the epilimnion. This is due to the fact that most of the water in the lake resides in the epilimnion, even when stratified. When the average masses of phosphorus at each stratum were added to determine mass for the total water column, there was a general increasing trend from early season to lake season (Fig. 22). Average September/October phosphorus mass is approximately 2.5X greater than the average April/May mass. The average September mass is approximately 3X greater than the April/May phosphorus mass.

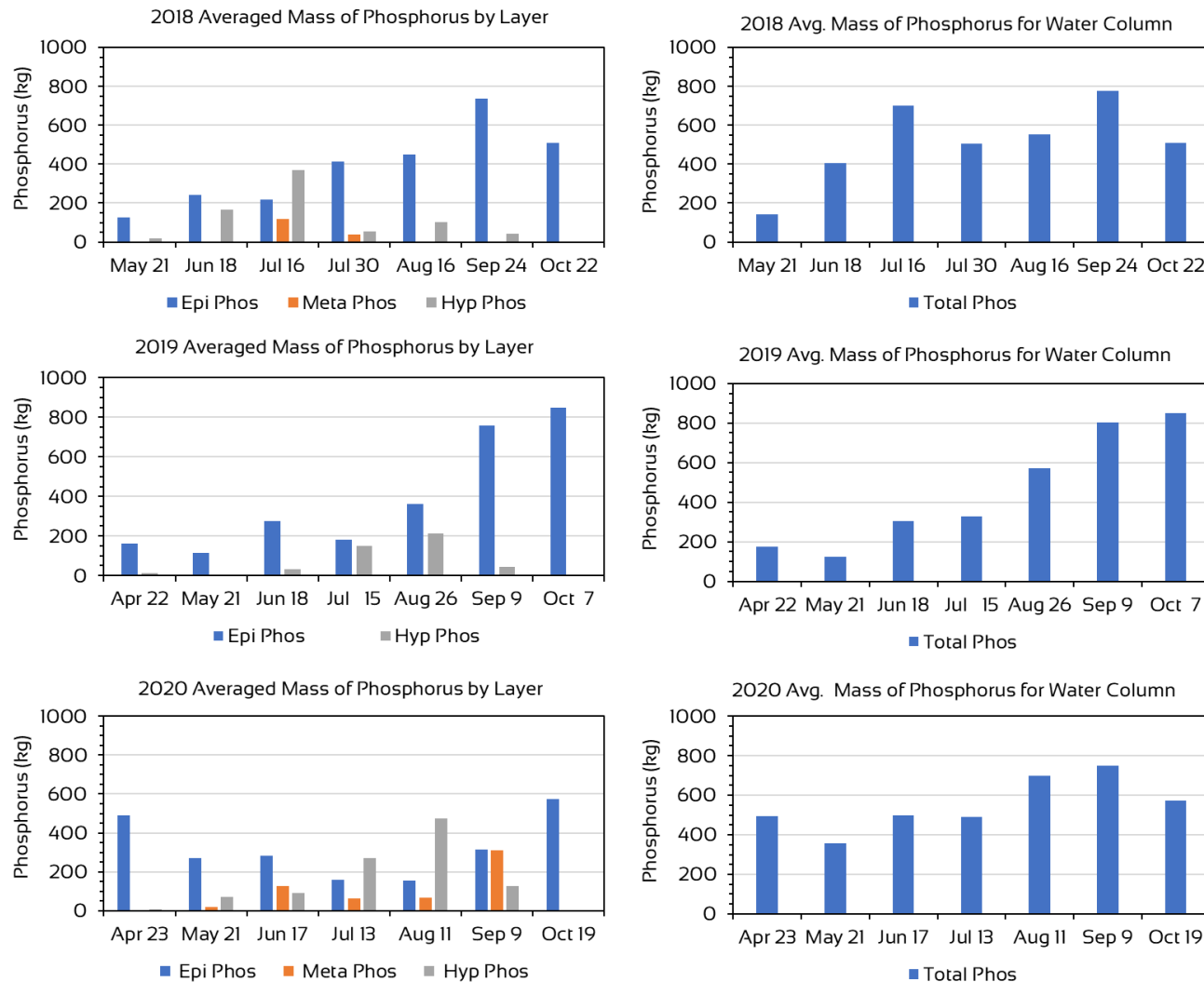


Figure 22. Results of analyses of the mass of phosphorus at each stratum of the water column (left) or for the entire water column (right) during the 2018, 2019, and 2020 sampling seasons.

Those approximations included an estimation of the phosphorus mass in April of 2018 which is not depicted in Fig. 22. On April 22, 2018 phosphorus concentrations in samples collected at 1m from the surface and 0.5m from the bottom of both the NB and CL sites were reported as not detectable. Concentrations in the middle of the water column were reported as 4 and 1µg/L at the NB and CL sites, respectively. The average concentration of 2.5µg/L multiplied by the volume of the lake in liters yielded a mass of 43.2kg.

### *Allochthonous Phosphorus and Cyanobacteria Dynamics*

While internal loading of (or *autochthonous*) phosphorus appeared to be important drivers of the Cyanobacteria bloom conditions for much of the season, those sources did not appear related to the *Aphanizomenon* bloom encountered on June 1<sup>st</sup>. The first signs of stratification were only observed on May 21<sup>st</sup>, and other indicators of loading from the sediments (e.g., low ORP, and high iron and phosphorus at the bottom of the water column) did not support an autochthonous source at that time.

We do note that early season (April/May) phosphorus concentrations were higher in 2020 than were observed in 2018 and 2019. In the 2020 April and May samples from all depths, phosphorus concentrations were between 27 and 30µg/L at the NB site; and between 30 and 40µg/L at the CL site. In 2018 and 2019 concentrations were between 4 and 19µg/L. Elevated concentrations in the early part of the season implicates *allochthonous* (watershed) sources of phosphorus and suggests this source is an important contributor to algal productivity early in the season.

### *Nitrogen, Limiting Nutrients, and Cyanobacteria*

The epilimnetic total nitrogen averages in 2020 were 448, 490, and 469µg/L for the NB and CL sites and entire lake, respectively. All averages were characteristic of mesotrophic productivity. The average for the NB site metalimnion was also within the mesotrophic range, while the hypolimnion average of 524µg/L was indicative of late mesotrophic conditions (Table 5). Late season concentrations in the NB hypolimnion did increase to eutrophic levels (Fig. 10).

Due to the protracted period of time of anoxia in the hypolimnion at the CL site, the season average concentration at that stratum (961µg/L) was significantly higher ( $p<0.05$ ) and characteristic of eutrophic conditions. Measured concentration in the later part of the season increased to highly eutrophic levels (Fig. 10).

Limnologists frequently used the Redfield ratio of 16 (16:1 of nitrogen to phosphorus) to determine whether nitrogen or phosphorus is limiting in a freshwater system (Redfield 1958). The ratio is based on moles and when converted to mass, 7.2µg/L is the ratio threshold which when under indicates nitrogen limitation while ratios above 7.2µg/L

indicate phosphorus limitations. The Redfield ratios were calculated for both the NB and CL sites and all depths for samples collected in April through October.

Redfield ratios were higher than 7.2 in the epilimnion and metalimnion on all dates at both sites (Table 6). On October 19th at the CL site, the metalimnion ratio was 7.4. Ratios at these strata were also lower (but not below 7.2) on April 23<sup>rd</sup>. The ratios in the hypolimnion of the NB site were all above 7.2, although they approached nitrogen limitation on July 13<sup>th</sup> and August 11<sup>th</sup> when hypolimnetic phosphorus were at their highest levels. In the CL hypolimnion, July 13<sup>th</sup> through September 9<sup>th</sup> ratios were below 7.2, and the others were low except the October 19<sup>th</sup> ratio.

Table 6. Redfield ratios in  $\mu\text{g/L}$  at the North Bay (NB) and Center Lake (CL) sites in the epilimnion (Epi), metalimnion (Meta), and hypolimnion in 2020.

Date	Epi TN:TP		Meta TN:TP		Hypo TN:TP	
	NB	CL	NB	CL	NB	CL
23-Apr	11.1	13.3	10.0	13.3	14.3	7.5
21-May	16.7	25.2	22.3	17.3	19.6	12.0
17-Jun	22.8	13.6	26.5	17.3	18.2	7.6
13-Jul	27.9	21.2	19.8	15.0	8.5	5.0
11-Aug	34.9	39.0	19.2	23.8	8.3	5.8
9-Sep	22.7	20.9	19.6	7.4	14.8	6.8
19-Oct	17.3	26.4	20.3	16.2	21.3	18.1

Nitrogen limitation favors many genera of Cyanobacteria because of their ability to utilize nitrogen that diffuses from the atmosphere into the water, whereas other taxa cannot. The site of nitrogen fixation, where atmospheric nitrogen ( $\text{N}_2$ ) is converted to ammonia ( $\text{NH}_3$ ), in some genera, e.g., *Dolichospermum spp.*, are specialized cells called heterocyst. Heterocysts were regularly observed in samples, particularly after mid-July. This suggests that during the periods in July when the lake was stratified and Cyanobacteria concentrations were highest near or below the thermocline, nitrogen fixation may have been important in meeting nutrient requirements.

### Other Environmental Factors and Cyanobacteria

High phosphorus concentrations, low total nitrogen to total phosphorus ratios, high pH, hard water, high concentrations of sodium, warm temperatures, and stable water columns with high resistant to mixing at the thermocline are some of the lake characteristics known to provide advantages to Cyanobacteria over other algal groups. A number of these variable have been discussed above in this report. Below we address several others.

Epilimnetic pH levels were often  $>8.2$  (Fig. 23) which provided an advantage to Cyanobacteria over other taxa. Above that threshold is when the dominant form of inorganic

carbon in the water shifts from carbon dioxide to bicarbonate. Cyanobacteria are capable of utilizing bicarbonate, whereas other taxa cannot.

Hypolimnetic pH levels at the NB, CL, and FP sites were never >8.2 except for an 8.4 measurement at the bottom of the FP site on September 21<sup>st</sup> when the water column was completely mixed. This suggested that there was no advantage to the Cyanobacteria for inorganic carbon requirements. The reason that the hypolimnetic pH values were lower was likely due to higher concentrations of CO<sub>2</sub> at the lower depths. At the SB site, hypolimnetic pH was on average higher (Fig. 23), and only exceeded 8.2 on September 21<sup>st</sup> when it was 8.9.

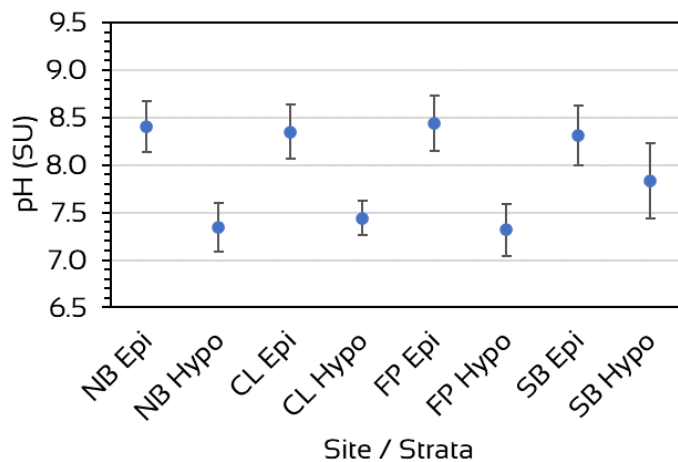


Figure 23. Epilimnetic and hypolimnetic pH averages for the 2020 season in the epilimnion (Epi) and hypolimnion (Hypo) of the North Bay (NB), Center Lake (CL), Folly Point (FP), and South Bay (SB) sites. Error bars represent one standard deviation.

We note that September 21<sup>st</sup> was the final time of the season pH data was collected in the field. pH data was not collected in October due to malfunctions of the pH probe. It is probably that as the water column mixed and Cyanobacteria were more equitably distributed, the pH at the lower depths would have been similar to levels measured at the surface.

Water temperatures of >25°C and water column stability favor surface bloom-forming Cyanobacteria for several reasons. Optimal temperatures for maximum Cyanobacteria growth are often >25°C, whereas growth rates for other taxa (e.g., diatoms) decline (Paerl and Otten 2012). Water temperatures of >25°C were consistently observed in the epilimnion from June 23<sup>rd</sup> through August 26<sup>th</sup>. Below the thermocline, temperatures were below 25°C.

Stability of a water column refers to the amount of mixing occurring. Mixing aids in maintaining many algae genera in the water column and preventing them from settling out. As mixing lessens and the water column becomes more stable, those taxa (e.g., Cyanobacteria) with effective adaptations to prevent them from settling out of the water column (e.g., buoyancy regulation) are favored over other taxa (e.g., diatoms) with less effective adaptations (e.g., maximizing surface to volume ratios). The increased temperature reduces water density thereby increasing settling of those algae with less effective means of remaining suspended in the water column.

As a water column becomes more stable, the resistance to mixing at the thermocline tends to increase in strength. RTRM scores of <30 mean that layers are mixed; scores of ≥30 between strata are characteristic of the transitional metalimnion layer. RTRM scores of ≥80 between strata characterizes strong resistance to mixing (Siver et.al. 2018). The maximum RTRM scores in the water column for all four sites were plotted to assess the stability of the water column during the 2020 season (Fig. 24).

While the SB site was observed to stratify, the maximum RTRM for the season was 71 and occurred on June 23<sup>rd</sup>. At the NB, CL, and FP sites, RTRM scores of ≥80 were consistently observed after June 1<sup>st</sup> through late July (Fig. 24). Strong resistance to mixing persisted through early-August at the FP site, and through mid-August at the CL site.

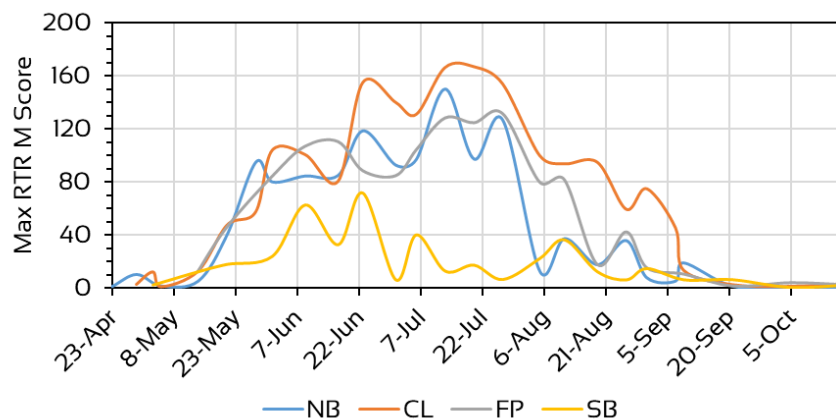


Figure 24. Maximum RTRM scores plotted over time in the water column of the North Bay (NB), Center Lake (CL), Folly Point (FP), and South Bay (SB) sites during the 2020 season.

Cyanobacteria have high ferrous iron ( $\text{Fe}^{2+}$ ) requirements relative to other eucaryotic algae taxa. Ferrous iron is that which results from the transformation of ferric iron ( $\text{Fe}^{3+}$ ) in the sediment via anaerobic cellular respiration. That transformation also results in the loading of phosphorus that was bound to the ferric iron. The loading of ferrous iron in the hypolimnion is believed to be one of the drivers of the migration down to or below the thermocline by the Cyanobacteria.

The loading of ferrous iron has been documented at Bantam Lake for the last three years. Hypolimnetic concentrations for all three years and both sites were plotted for comparative purposes (Fig. 25). The concentration in June of 2020 of the CL site was notably higher than the June concentration in 2018 and 2019. The 2019 and 2020 July concentrations were similar and greater than the 2018 July concentration. The August 2020 hypolimnetic concentration was the greatest over the three-year period (2019 August through October data was not collected).



The reduction of ferric iron to ferrous iron is a consequence of anoxic conditions for a period of time long enough to first utilize other oxidizing compounds, e.g., nitrate and manganese. Differences in hypolimnetic iron concentrations may be due to differences in seasonal patterns of stratification, e.g., if a lake stratifies earlier or quicker, then processes that occur in aquatic anaerobic environments may occur sooner.

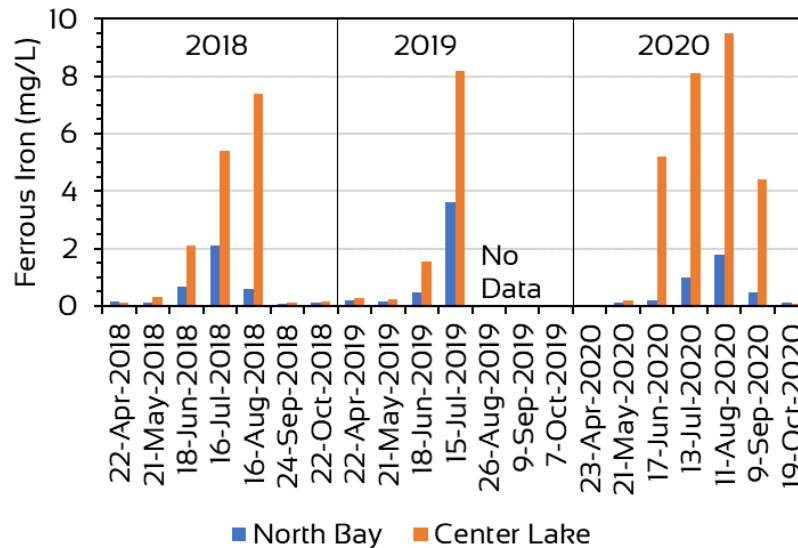


Figure 25. Ferrous iron concentrations in the hypolimnion of the North Bay and Center Lake sites in the 2018, 2019, and 2020 seasons. Data not available for August 26 – October 7, 2019.

## RECOMMENDATIONS

1. Bantam Lake has a high degree of water contact recreational activity, and is also one where management of several aquatic invasive plants and Cyanobacteria occur. For these reasons, the continuation of the monthly water quality monitoring and biweekly Cyanobacteria monitoring programs are advised to ensure informed decision-making on recreational use and to assess impacts of management activities on water quality.
2. Current sampling protocols (i.e., integration of top three meters of the water column) maybe underestimating Cyanobacteria cell concentrations, relative phycocyanin concentrations, microcystin concentrations, and chlorophyll-*a* concentrations when surface blooms are visible.

- a. To resolve underestimations of relative phycocyanin, future data collections with the multiprobe should start with a measure of all parameters at the surface and not 0.5 meters.
  - b. To resolve underestimations of Cyanobacteria cell concentrations, sample collections should be based on visual assessments and relative phycocyanin data. If a surface bloom is present, samples should be collected at the surface for cell counts and microcystin analyses. If relative phycocyanin concentrations are similar in the top 3m, then the integrated sample is still appropriate.
  - c. Until further investigations are complete, we do not recommend modifying sample collections for chlorophyll-*a* analyses.
3. The BLPA is currently collaborating with the CT DEEP on the development of a TMDL and watershed management plan. Our data (e.g., spring epilimnetic total phosphorus concentrations and early June algae bloom) support this need and we recommend continued efforts there.
4. This year and last we documented loading of phosphorus from the sediments after the lake stratified and anoxic conditions developed at strata near the bottom. We believe management of this source of nutrients requires management.



## REFERENCES

- Bell, M. 1985. The Face of Connecticut. State Geological and Natural History Survey of Connecticut. Bull. 110.
- Canavan RW, Siver PA. 1994. Chemical and physical properties of Connecticut lakes, with emphasis on regional geology. LAKE RESERV MANAGE. 10(2):175-188.
- Canavan RW, Siver PA. 1995. Connecticut Lakes: A study of the chemical and physical properties of fifty-six Connecticut Lakes. New London (CT): Connecticut College Arboretum.
- Connecticut Department of Energy and Environmental Protection (CT DEEP). 1991. Trophic Classifications of Forty-nine Connecticut Lakes. CT DEEP, Hartford, CT. 98 pp.
- Connecticut Department of Public Health and Connecticut Department of Energy and Environmental Protection. 2019. Guidance to Local Health Departments for Blue–Green Algae Blooms in Recreational Freshwaters. See [https://portal.ct.gov/-/media/Departments-and-Agencies/DPH/dph/environmental\\_health/BEACH/Blue-Green-AlgaeBlooms\\_June2019\\_FINAL.pdf?la=en](https://portal.ct.gov/-/media/Departments-and-Agencies/DPH/dph/environmental_health/BEACH/Blue-Green-AlgaeBlooms_June2019_FINAL.pdf?la=en)
- Deevey ES Jr. 1940. Limnological studies in Connecticut. V. A contribution to regional limnology. AM J SCI. 238(10):717-741.
- Frink CR, Norvell WA. 1984. Chemical and physical properties of Connecticut lakes. New Haven (CT): Connecticut Agricultural Experiment Station. Bulletin 817. 180 pp
- Healy DF and KP Kulp. 1995. Water Quality Characteristics of Selected Public Recreational Lakes and Pond in Connecticut. US Geological Survey Water-Resource Investigations Report 95-4098. 227pp.
- Jacobs RP, O'Donnell EB. 2002. A fisheries guide to lakes and ponds of Connecticut, including the Connecticut River and its coves. Hartford (CT): Connecticut Department of Energy and Environmental Protection, Bulletin No. 35.
- Lawton L., Marsalek B., Padisák J., Chorus I. 1999. DETERMINATION OF CYANOBACTERIA IN THE LABORATORY. In Toxic Cyanobacteria in Water: A guide to their public health consequences, monitoring and management. Chorus and Bartram, eds.
- McMaster NL & DW Schindler. 2005. Planktonic and Epipellic Algal Communities and their Relationship to Physical and Chemical Variables in Alpine Ponds in Banff National Park, Canada, Arctic, Antarctic, and Alpine Research, 37:3, 337-347, DOI: 10.1657/1523-0430(2005)037[0337:PAEACA]2.0.CO;2
- Paerl, H.W. & Otten, T.G. 2013. Harmful cyanobacterial blooms: causes, consequences and controls. Microb. Ecol. 65, 995–1010.
- Redfield A.C. 1958. The biological control of chemical factors in the environment. American Scientist. 46(3):205-221.
- Siver PA .1992. Assessing historical conditions of Bantam Lake, Connecticut, using a paleolimnological technique. Report to the Town of Morris, Connecticut
- Siver, P.A. 1993. Inferring lakewater specific conductivity with scaled chrys-phytes. Limnol. Oceanogr. 38: 1480-1492



Siver, P.A., Ricard, R., Goodwin, R. and A.E. Giblin. 2003. Estimating historical in-lake alkalinity generation and its relationship to lake chemistry as inferred from algal microfossils. *J. Paleolimn.* 29: 179-197.

Siver PA & Marsicano LJ. 1996. Inferring lake trophic status using scaled chrysophytes. In: *Chrysophytes: Progress and New Horizons*. Kristiansen J, Cronberg G (eds) Beihefte zur Nova Hedwigia 114: 233-246

Siver P., Marsicano L., Lott A., Wagener S., Morris N. 2018. Wind induced impacts on hypolimnetic temperature and thermal structure of Candlewood Lake (Connecticut, U.S.A.) from 1985–2015. *Geo: Geography and the Environment*. 5(2). <https://doi.org/10.1002/geo2.56>

Søndergaard, M., 2009. Redox Potential. In *Encyclopedia of Inland Waters* ed. Gene Likens. Academic Press.

Wetzel RG. 2001. *Limnology Lake and River Ecology*. 3<sup>rd</sup> Ed. Academic Press. 1006 pp.

